

APPENDIX G

RESUSPENSION, DEPOSITION, AND TRANSPORT OF
FINE-GRAINED SEDIMENTS IN RIVERS AND NEAR-SHORE AREAS

INTERIM REPORT

Resuspension, Deposition and Transport of Fine-Grained Sediments
in Rivers and Near-Shore Areas

by

Wilbert Lick

Kirk Ziegler

Cheng-Hui Tsai

Department of Mechanical and Environmental Engineering
University of California
Santa Barbara, CA 93106

September, 1987

Abstract

A quantitative knowledge of the resuspension, deposition, and transport of fine-grained sediments is essential in understanding and predicting the fate of contaminants in aquatic systems and has been the justification for much of our recent research. In the present report, recent work on this subject is discussed. Three distinct but related investigations are presented. These are: (1) numerical modeling of the transport of fine-grained sediments in shallow waters; (2) a sediment resuspension study in the Detroit River; and (3) the flocculation of fine-grained sediments due to a uniform shear stress.

These three investigations and related work greatly enhance our understanding of fine-grained sediments. With some additional work on the aggregation and disaggregation of these sediments, a quantitative description of the resuspension, deposition, and transport of fine-grained sediments is now feasible.

Of course, the ultimate goal of this and related research is to understand and quantitatively predict the transport and fate of contaminants. Of importance in this overall process is (a) the resuspension and deposition of sediments, (b) the aggregation and disaggregation of sediments, and (c) the interfacial processes which determine the phase/speciation of a contaminant either in suspension or in the bottom sediments. These are all interactive processes.

Specific tasks which are necessary to quantitatively understand these processes and their interaction are discussed in the present report. Completion of these tasks will allow us to quantitatively describe the fluxes of contaminants due to the resuspension of bottom sediments.

Acknowledgements

These studies were supported by the United States Environmental Protection Agency. Dr. Tony Kizlauskas, Mr. Bill Richardson, and Dr. Louis Swaby were the project officers.

Contents

	Page
Introduction-----	4
Conclusions and Recommendations-----	10
Numerical Modeling of the Transport of Fine-Grained Sediments	17
A Sediment Resuspension Study in the Detroit River-----	40
The Flocculation of Fine-Grained Lake Sediments Due to a Uniform Shear Stress-----	59
References-----	91

INTRODUCTION

A major fraction of the sediments in the Great Lakes and the near-shore areas of the oceans are fine-grained (less than 60 μm in diameter). For example, in Lake Erie, 90% of the surficial sediments are in this category. Fine-grained sediments have relatively large surface to mass ratios compared to coarse-grained sediments and therefore have relatively large adsorptive capacities. For this reason, many contaminants are readily adsorbed onto fine-grained sediments and are transported with them.

Because of this adsorption, bottom sediments are a major repository of contaminants and they serve as a highly variable source or sink for contaminants in the overlying water. This flux of contaminants from the bottom sediments into the overlying water depends on (a) the resuspension and deposition of bottom sediments due to currents, tides, and wave action, (b) benthic activity, and (c) chemical diffusion. In shallow areas, the resuspension and deposition of bottom sediments is the primary cause of contaminant flux from the bottom sediments to the overlying water.

A quantitative knowledge of the resuspension, deposition, and transport of fine-grained sediments is essential in understanding and predicting the fate of contaminants in aquatic systems and has been the justification for much of our recent research. This research has involved laboratory and field investigations as well as theoretical and numerical modeling. The primary emphasis has been on transport processes in shallow waters, e.g., rivers, harbors, shallow lakes, and near-shore areas of the oceans.

In the present report, recent work on the resuspension, deposition, and transport of fine-grained sediments is discussed. Three distinct but related investigations are presented. These are: (1) numerical modeling of the

transport of fine-grained sediments in shallow waters; (2) a sediment resuspension study in the Detroit River; and (3) the flocculation of fine-grained sediments due to a uniform shear stress.

In the first study, a numerical model of the resuspension, deposition, and transport of fine-grained, cohesive sediments was developed and applied. The model is quite general and can treat variable geometry and bottom depth as well as a wide range of boundary conditions. An essential part of this model is an accurate and physically realistic description of the sediment bed and the resuspension of the bottom sediments due to physical processes such as currents, tides, and wave action. The description of the sediment bed is based on recent experimental and field results for fine-grained sediments (Lee et al., 1981; Lick, 1982; Lick and Kang, 1987; MacIntyre et al., 1986; Tsai and Lick, 1987). In particular, these experiments have demonstrated that at a particular stress the resuspension rate for fine-grained, cohesive sediments decreases with time such that only a fixed amount of sediment can be resuspended over a long period of time. This is in contrast to uniform-size, non-cohesive sediments where the resuspension rate is approximately constant with time. Resuspension rates and the net amount of material that can be resuspended have been determined as a function of applied shear stress and time after deposition for various fine-grained sediments. Pertinent results have been incorporated into the present model and, from this, the changes in the resuspension properties of the sediment bed with time due to resuspension, deposition, and compaction can be approximately predicted.

The basic equations of motion governing the transport of fluid and sediment are three-dimensional and time-dependent. Numerical calculations have been made with these equations but are time-consuming and cumbersome.

In order to simplify the analysis, reduce computational costs and time, and hence be able to investigate sediment transport more readily, a vertically integrated model has been developed and used. The major assumption for the model to be valid is that the water column is thoroughly mixed in the vertical direction, a reasonable approximation for many shallow waters.

In many hydrodynamic and sediment transport problems of practical interest, the body of water being considered (for example, a river, bay, or harbor) is connected to a larger body of water such as a lake or ocean. A computational boundary must be placed somewhere in the lake or ocean in order to keep the number of grid points used in the calculation at a practical level. Disturbances which are generated within the region must propagate through this open boundary without significant reflection or distortion. More generally, prescribed exterior disturbances or forcings such as those due to currents, tides, or storm surges may be present and influence the interior solution while the interior disturbances must again propagate out of the region without reflection at the boundary. Numerically modeling the conditions at this open boundary has been a difficult problem in the past. In the calculations presented here, a procedure developed by us (Lick et al., 1986, 1987) has been used to successfully treat this problem.

The model has been applied to the resuspension, deposition, and transport of fine-grained sediments in (a) the Raisin River, a small polluted stream flowing into Lake Erie; (b) a river flowing into a lake or ocean with a cross-flow; and (c) a time-dependent flow in a simple estuary as affected by tidal currents (Ziegler and Lick, 1987, 1988). Additional examples, the governing differential and difference equations, and the details of the numerical procedure can be found in a report by Ziegler and Lick (1986).

In order to quantitatively predict sediment transport, one must know the net flux of sediments at the sediment-water interface. It is well known that sediment properties, the resuspension rate in particular, vary widely (by orders of magnitude) throughout a system and with time at one location. Laboratory experiments (Partheniades, 1965; Mehta and Partheniades, 1975; Fukuda and Lick, 1980; Lee et al, 1981; Lick 1982) have determined the dependence of resuspension rates on various governing parameters such as applied shear stress, water content or time after deposition, particle size distribution, mineralogy, water chemistry, and numbers and types of benthic organisms. However, the state of the sediments in situ are not well known and so the art of extrapolating laboratory results to the field is not well developed. A further disadvantage of laboratory resuspension experiments is that they are cumbersome and very time-consuming.

In order to alleviate some of these difficulties, a portable device for the rapid measurement of sediment resuspension (called a shaker) has been developed (Tsai and Lick, 1986). It can be used in the laboratory for quick and reasonably accurate measurements of resuspension but, more importantly, it can be used on board ship for rapid surveys of the resuspension of relatively undisturbed sediments throughout an aquatic system. This device essentially measures the total amount of sediment resuspended at a particular stress. This data can then be used directly in our numerical model described above.

By means of this device, we have measured sediment resuspension at various locations in Lake St. Clair (Tsai and Lick, 1986) and in the Detroit River. Results of this latter investigation are presented as the second study in the present report.

Flocculation has a significant effect on the effective sizes, surface areas, densities, settling velocities, and deposition rates of fine-grained sediments and hence is important in determining the transport and fate of not only sediments but contaminants as well. It should be emphasized that flocculation is a dynamic process with both aggregation and disaggregation of particles occurring continuously.

The effects of fluid shear on the rate of aggregation and disaggregation of fine-grained sediments are of major importance in lakes but are not well understood. In the study presented here, experiments were performed to investigate these effects. A Couette viscometer was used to apply a uniform shear stress to the sediment suspension. A series of experiments were made for shear stresses of 1, 2, and 4 dynes/cm² and for sediment concentrations from 50 mg/l to 800 mg/l, values which are characteristic of those found in the Great Lakes.

The particle size distribution as a function of time was determined. Quantitative results were obtained for the decrease in steady-state floc size with increasing shear stress and with increasing sediment concentration. For example, the steady-state median floc diameter changed from 100 μ m to 50 μ m as the shear stress changed from 1 dyne/cm² to 4 dynes/cm² (when the sediment concentration was 100 mg/l) and changed from 100 μ m to 25 μ m as the sediment concentration changed from 50 mg/l to 800 mg/l (when the shear stress was constant at 2 dynes/cm²). The times required for flocculation to occur under different conditions were also determined and were typically on the order of an hour, again dependent on the shear and sediment concentration.

Experiments were performed such that the steady-state was approached in different ways. It was found that the steady state particle size distribution was independent of its history. Of course, this makes a theoretical analysis involving flocculation much easier.

An analysis of these experimental results is continuing (publication in preparation). From this analysis, it can be shown that the effects of pure shear on disaggregation is minimal while the effects of collisions between particles (possibly due to shear but also due to differential settling and Brownian motion) is the dominant mechanism for disaggregation. A general formula for the time rate of change of the particle size distribution and approximate values for the coefficients appearing in this equation have been determined from the experimental results. It can be shown that these coefficients are strong functions of the floc diameter, shear stress, and concentration. In general, good agreement between the theory and the experimental results has been obtained.

CONCLUSIONS AND RECOMMENDATIONS

The major objective of our recent research has been to develop a quantitative, predictive understanding of the transport of fine-grained sediments and of contaminants adsorbed to these sediments. This has involved laboratory and field investigations as well as theoretical and numerical modeling.

As part of our research, we have done extensive experimental work on the resuspension and deposition of fine-grained cohesive sediments from rivers and lakes. In particular, the resuspension rates and the net amount of sediment that can be resuspended at a particular stress have been determined as a function of applied shear stress and time after deposition for various sediments from the Great Lakes. This data has been used to develop a physically realistic description and numerical model of the sediment bed and the flux of sediments from this bed. From this, changes in the sediment bed with time due to resuspension, deposition, and compaction can be determined.

This information has been incorporated into a hydrodynamic and sediment transport model. In this model, the sediment bed is approximated by layers in each of which the properties are independent of depth but may vary with time. The model can also treat conditions at open boundaries accurately and realistically. The model has been applied to several typical problems concerned with the resuspension, deposition, and transport of fine-grained sediments. Erosional and deposition features that are commonly observed in these flows were reproduced. By means of the model, the parameters on which these features depend can be accurately determined. Steady and time-dependent flows can be analyzed.

The model is relatively easy to use and is valid over a wide range of conditions. It should be especially useful for shallow near-shore areas, where contaminant release and transport is of the utmost importance. For these purposes, in situ sediment resuspension properties are needed as input to the model. These can most easily be determined by use of a recently developed portable device (the shaker) whereby rapid and reasonably accurate surveys of the resuspension properties of bottom sediments can be made. By means of this device, we have measured sediment resuspension at various locations in Lake St. Clair and in the Detroit River.

It should be noted that sediment entrainment and other properties of sediments change drastically from one location to another and also change drastically with time at one location depending on parameters which in turn are heavily dependent upon environmental conditions. Because of this, although the sediment properties may be known at one time, it is extremely difficult to predict the properties of these sediments at a later time, for example, after a storm which may cause large transport and hence large changes in the properties of the sediments. One solution of course is to continuously measure sediment properties throughout the system. This is prohibitive in time and cost. A more reasonable solution is (a) to use the shaker and similar instrumentation to survey the sediment properties in situ at reasonable time intervals, (b) use laboratory experiments to determine the changes of the sediment properties due to the parameters on which the properties depend, and (c) then combine these two types of information by means of our numerical model so as to have a better understanding of in situ conditions and how they vary with time under specified environmental conditions.

Flocculation has a significant effect on the effective sizes, surface areas, densities, settling velocities, and deposition rates of fine-grained sediments and hence is important in determining the transport and fate of not only sediments but contaminants as well. In the study presented here, experiments were performed to investigate the influence of fluid shear on flocculation. A Couette viscometer was used to apply a uniform shear stress to the sediment suspension. A series of experiments were made for shear stresses of 1, 2, and 4 dynes/cm² and for sediment concentrations of 50 mg/l to 800 mg/l, values which are characteristic of those found in the Great Lakes.

The particle size distribution as a function of time was determined. Quantitative results were obtained for the decrease in steady-state floc size with increasing shear stress and with increasing sediment concentration. For example, the steady-state median floc diameter changed from 110 μm to 50 μm as the shear stress changed from 1 dyne/cm² to 4 dynes/cm² (when the sediment concentration was 100 mg/l) and changed from 100 μm to 25 μm as the sediment concentration changed from 50 mg/l to 800 mg/l (when the shear stress was constant at 2 dynes/cm²). The times required for flocculation to occur under different conditions were also determined and were typically on the order of an hour, again dependent on the shear and sediment concentration.

A theoretical analysis of these results is presently being made. In particular, a general formula for the time rate of change of the particle size distribution and approximate values for the coefficients appearing in this equation have been determined. Good agreement between the theory and the experimental results has been obtained.

The work described above greatly enhances our understanding of the resuspension, deposition, and transport of fine-grained sediments. Addi-

tional work on the aggregation and disaggregation of these sediments is needed before the effects of flocculation on the transport of fine-grained sediments can be adequately understood and quantitatively predicted. This additional work is described below along with other recommended research.

The ultimate goal of this and related research is to understand and quantitatively predict the transport and fate of contaminants. As indicated earlier, a major source of contaminants to the overlying water is the flux from the bottom sediments. This flux is due to (a) resuspension of the bottom sediments due to wave action and currents followed by re-equilibration of partitioned solutes, (b) benthic activity of bottom dwelling organisms which enhances mixing of the surficial bottom sediments, and (c) molecular diffusion. Of these three, resuspension is generally the largest and in shallow waters is often several orders of magnitude greater than the other two.

In determining the flux of contaminants due to resuspension, one must consider various interacting physical and chemical processes. These include the resuspension and subsequent deposition of the particulate matter, the aggregation and disaggregation of the suspended sediments, and the interfacial processes which determine the phase/speciation of a contaminant either in suspension or in the bottom sediments.

The tasks listed below are necessary to quantitatively understand these processes. Their completion will allow us to quantitatively describe the fluxes of contaminants due to the resuspension of bottom sediments.

These tasks have been discussed thoroughly with the Clarkson Three (DePinto, Theis, and Young) and are joint recommendations by researchers here at UCSB and at Clarkson.

1. Aggregation-Disaggregation Experiments

The purpose of this set of experiments is to thoroughly understand and characterize the physical and chemical processes affecting the aggregation and disaggregation of fine-grained sediments.

1.1 Viscometer experiments. Experiments using a Couette viscometer should be continued in order to determine the effects of fluid shear and water chemistry on the aggregation and disaggregation of sediments. Experimental variables should include sediment concentration, shear stress, and basic water chemistry (such as pH, ionic strength, and contaminant level).

1.2 Settling studies. Because of flocculation, settling velocities are not uniquely related to particle sizes. Settling velocities should be measured directly using (a) a microscope and camera, and/or (b) laser doppler velocimetry. The relation between particle size distribution and settling velocities should be determined as a function of shear stress, sediment concentration, and water chemistry.

1.3 Annular flume experiments. When cohesive sediments are resuspended, they are resuspended as flocs or clumps of particles rather than as individual particles. This size distribution is then modified as a function of time due to shear stresses in the overlying water. Resuspension experiments to describe this process should be done. The size distribution of the suspended particles should be measured as a function of time. This is essential in the description of contaminant release from suspended sediments because of the potential for a considerable variation in sorbent surface area during the process (see section 2).

2. Chemical Release Experiments

The purpose of these experiments is to thoroughly understand and characterize the release (or uptake) of contaminants as bottom sediments are resuspended and later deposited.

2.1 Viscometer experiments. The viscometer provides a very well controlled experimental device to study the effect of shear stress on the rate of contaminant release or uptake by particulate matter. If shear-induced changes in particle size distribution cause adsorption or desorption to occur, its rate can be measured in this device. Even when the particle size distribution does not change significantly, the ability to perform adsorption or desorption experiments at a constant average fluid shear at the particle surface will permit assessment of the extent to which diffusion processes control the uptake or release rate.

In these experiments the experimental variables should be sediment concentration, shear stress; time under constant shear, contaminant and its concentration, macro water chemistry (e.g. pH, ionic strength, DOC), and sorption time prior to application of shear.

2.2 Annular flume experiments. Resuspension and deposition experiments using flumes should be conducted in such a way as to simulate all the above processes simultaneously under carefully controlled laboratory conditions. In addition to solid dynamics, contaminant phase/speciation changes should be measured as a function of time for various shear stresses and initial sediment contaminant concentrations. These experiments will provide an excellent means to parameterize and calibrate a mathematical model of sediment transport-contaminant exposure for this phenomenon. The annular flume is unique in that it permits evaluation of both the short-term, transition period between initiation of resuspension and attainment of steady-state

suspended solids in the overlying water and the longer-term, steady-state period during which the slower contaminant-particle reactions continue to occur.

2.3 Field shaker experiments. Experiments similar to those above should be done using our portable device for measuring sediment resuspension. The shaker is a useful device for making measurements in the field. The experiments would be used to compare results from the flumes and the shaker and hence verify the shaker results. After verification, the shaker could be used for field surveys to study sediment resuspension and contaminant release as a function of location and environmental conditions. It should be noted, however, that the shaker device can only be used to capture the transition particle and contaminant dynamics, hence an additional reason for work in the annular flume.

3. Mathematical Model Development

The above experiments will lead to the development of a mathematical model of sediment transport and contaminant transport/transformation during a resuspension event. Essential components of this model will be (a) the rates of resuspension and deposition and the associated particle size distribution; (b) the rates of aggregation and disaggregation; (c) the settling velocity distributions; and (d) the rates and extent of sorption/desorption reactions in the resuspension medium. These quantities need to be determined throughout the system as a function of position and time. The experiments described above will permit the simulation of these processes given knowledge of certain fundamental, measurable parameters of a given ecosystem.

THE TRANSPORT OF FINE-GRAINED SEDIMENTS IN SHALLOW WATERS

In an effort to understand and quantitatively predict the transport of fine-grained sediments and the contaminants associated with them, a numerical transport model has been developed. An essential part of this model is an accurate and physically realistic description of the sediment bed and the resuspension of the bottom sediments due to physical processes such as currents, tides, and wave action. The description of the sediment bed is based on recent experimental and field results for fine-grained sediments (Lee et al., 1981; Lick, 1982; Lick and Kang, 1987; MacInyre et al., 1986; Tsai and Lick, 1988). In particular, these experiments have demonstrated that at a particular stress the resuspension rate for fine-grained, cohesive sediments decreases with time such that only a fixed amount of sediment can be resuspended over a long period of time. This is in contrast to uniform-size, non-cohesive sediments where the resuspension rate is approximately constant with time. Resuspension rates and the net amount of material that can be resuspended have been determined as a function of applied shear stress and time after deposition for various fine-grained sediments. Pertinent results have been incorporated into the present model and, from this, the changes in the resuspension properties of the sediment bed with time due to resuspension, deposition, and compaction can be approximately predicted. Sediment dynamics are discussed in more detail in the following section.

The basic equations of motion governing the transport of fluid and sediment are three-dimensional and time-dependent. Numerical calculations have been made with these equations but are time-consuming and cumbersome. In order to simplify the analysis, reduce computational costs and time, and

hence be able to investigate sediment transport more readily, a vertically integrated model has been developed and used. The major assumption for the model to be valid is that the water column is thoroughly mixed in the vertical direction, a reasonable approximation for many shallow waters.

In many hydrodynamic and sediment transport problems of practical interest, the body of water being considered (for example, a river, bay, or harbor) is connected to a larger body of water such as a lake or ocean. A computational boundary must be placed somewhere in the lake or ocean in order to keep the number of grid points used in the calculation at a practical level. Disturbances which are generated within the region must propagate through this open boundary without significant reflection or distortion. More generally, prescribed exterior disturbances or forcings such as those due to currents, tides, or storm surges may be present and influence the interior solution while the interior disturbances must again propagate out of the region without reflection at the boundary. Numerically modeling the conditions at this open boundary has been a difficult problem in the past. In the calculations presented here, a procedure developed by us (Lick and others, 1986, 1987) has been used to successfully treat this problem. The numerical model and the treatment of the open boundary condition are discussed in more detail in the third section.

The model has been applied to the resuspension, deposition, and transport of fine-grained sediments in (a) the Raisin River, a small polluted stream flowing into Lake Erie; (b) a river flowing into a lake or ocean with a cross-flow; and (c) a time-dependent flow in a simple estuary as affected by tidal currents (Ziegler and Lick, 1987, 1988). These examples are discussed in the fourth section. Additional examples, the governing differential and difference equations, and the details of the numerical procedure can be found in a report by Ziegler and Lick (1986).

Sediment Dynamics

A necessary parameter in the quantitative numerical modeling of sediment transport is the sediment flux at the sediment-water interface. This net flux q_s ($\text{gm}/\text{cm}^2\text{-s}$) can be written as the difference between the resuspension (entrainment) rate E and the deposition rate D , or $q_s = E - D$. The fact that real sediments are a mixture of particles with widely varying size and composition has a significant effect on both E and D and hence q_s . For example, for a typical suspended sediment, particle diameters may vary from less than one micrometer to several hundred micrometers (or over three orders of magnitude) while settling speeds may vary by more than four orders of magnitude.

For particles of a single size, the deposition rate can be written as $D = \beta C$ where C is the sediment concentration (gm/cm^3) and β is a coefficient with units of velocity. The value of β is dependent on Brownian motion, turbulent diffusion, and settling near the sediment-water interface (Lick and Kang, 1987). However, for particles greater than about $1 \mu\text{m}$ in diameter, β is primarily dependent on settling and is approximately equal to the settling speed. For mixtures of particles, it is assumed that $D = \sum_m \beta_m C_m$ where the mixture has been separated into components each with its own concentration C_m and settling speed β_m .

The flocculation of fine particles has a significant and dynamic effect on the effective sizes, densities, and settling speeds of the resulting aggregates of particles, or flocs. Laboratory experiments have been and are being conducted to understand and determine the rates of aggregation and disaggregation of flocs and the parameters on which they depend (see, for example, Ives, 1978; Hunt, 1982; Tsai et al., 1987). Experimental and theoretical work on flocculation is continuing in our laboratory and should

lead to a reasonably quantitative description of flocculation in the near future. However, at the present time, the data is still insufficient to formulate a quantitative model of flocculation. For this reason, the dynamic effects of flocculation have been ignored in the present calculations and the sediments are separated into non-interacting components each with its own average size and settling speed.

The resuspension rate E is significantly affected by particle size variations and also by cohesion between particles. At low stresses, only the finer particles on the surface of the bed can be resuspended while the larger particles are left behind and armor the bed. In addition, cohesion of particles and the resulting compaction of the bed cause E to vary with time after deposition and with depth. Because of this, sediments near the surface are less compacted and are relatively easy to resuspend while sediments further down are more compacted and more difficult to resuspend. The result of all of this is that, for fine-grained sediments at any particular stress, only a finite and relatively small amount of sediment can be resuspended as opposed to non-cohesive, uniform-size sediments which have a uniform rate of resuspension.

Experimental work (Lee and others, 1981; Lick and Kang, 1987; MacIntyre and others, 1986) has determined the dependence of the resuspension rate E and the total amount of sediment ϵ (gm/cm^2) that can be resuspended at a particular stress as a function of (a) the turbulent stress at the sediment-water interface, and (b) the water content of the deposited sediments (or the time after deposition) for various sediments from both lakes and oceans. A formula for ϵ which approximates this data can be written as

$$\begin{aligned} \varepsilon &= a \left[\frac{\tau - \tau_0}{\tau_0} \right]^m && \text{for } \tau \geq \tau_0 \\ &= 0 && \text{for } \tau < \tau_0 \end{aligned} \quad (1)$$

where ε is the net amount of resuspended sediment per unit surface area in gm/cm^2 , $a = a_0/t_d^n$, a_0 is approximately equal to 8×10^{-3} , both n and m are approximately equal to two, t_d is the time after deposition in days, τ is the shear stress (dynes/cm^2) produced by wave action and currents, and τ_0 is an effective critical stress generally on the order of 1 dyne/cm^2 . Each of the parameters τ_0 , a_0 , n and m is dependent on the particular sediment and needs to be determined experimentally. However, for fine-grained sediments, the values given above are a reasonably accurate first approximation.

The above formula, Eq. (1), is for the net resuspension. The total amount of sediment is not resuspended instantaneously but over a period of time on the order of an hour. In numerical computations, a reasonable approximation to the resuspension rate is that E is constant and equal to its initial value until all available sediment is resuspended and is then zero until further sediment is deposited and is available for resuspension.

The sediment bed, which in reality has a continuous variation of properties with depth, is approximated by layers in each of which the properties are independent of depth within the layer but may vary with time as described by the equation above. In the present calculations, three layers were used. The amount of material in the surface layer is modified by the deposition of suspended sediments to that layer and resuspension of sediments from that layer.

Sediments that are deposited on the bed within the first day after the calculation has begun are assumed to have a time after deposition of one day. If the sediment layer originally present at the top of the bed has a time

after deposition of one day, the newly deposited sediment is simply added to that layer. If the time after deposition of the top layer is greater than one day, a new top layer is formed from the newly deposited sediment.

Resuspension of sediments occurs when the shear stress due to currents exceeds the critical shear stress of the sediments. The amount of sediment resuspended during one time step is then $\Delta\varepsilon = E\Delta t$. This applies until the amount of sediment resuspended is equal to ε , the maximum amount of sediment that can be resuspended from that layer for a particular stress, or until the entire layer is resuspended.

A Vertically-Integrated Transport Model

In the present model, vertically-integrated hydrodynamic and sediment transport equations have been used in order to simplify the analysis. The assumptions inherent in this model are: the pressure varies hydrostatically, the water column is thoroughly mixed in the vertical direction, and the horizontal velocities and suspended sediment concentrations are approximately independent of depth. The resulting hydrodynamic equations are:

$$\frac{\partial \eta}{\partial t} + \frac{\partial U}{\partial x} + \frac{\partial V}{\partial y} = 0 \quad (2)$$

$$\frac{\partial U}{\partial t} + gh \frac{\partial \eta}{\partial x} = \tau_x^W - \tau_x^B + A_H \left(\frac{\partial^2 U}{\partial x^2} + \frac{\partial^2 U}{\partial y^2} \right) - \frac{\partial}{\partial x} \left(\frac{U^2}{h} \right) - \frac{\partial}{\partial y} \left(\frac{UV}{h} \right) \quad (3)$$

$$\frac{\partial V}{\partial t} + gh \frac{\partial \eta}{\partial y} = \tau_y^W - \tau_y^B + A_H \left(\frac{\partial^2 V}{\partial x^2} + \frac{\partial^2 V}{\partial y^2} \right) - \frac{\partial}{\partial x} \left(\frac{UV}{h} \right) - \frac{\partial}{\partial y} \left(\frac{V^2}{h} \right) \quad (4)$$

where the total water depth $h = h_0 + \eta$, $h_0(x,y)$ is the equilibrium water depth (cm), $\eta(x,y)$ is the surface displacement from that equilibrium, U and V are vertically integrated velocities (cm^2/s) defined by

$$U = \int_{-h_0}^{\eta} u \, dz, \quad (5)$$

$$V = \int_{-h_0}^{\eta} v \, dz, \quad (6)$$

u and v are velocities (cm/s) in the x and y directions respectively, z is the vertical coordinate, τ^w is the wind stress (dynes/cm²), τ^B is the bottom stress whose components are given by $\tau_x^B = c_f u|u|$ and $\tau_y^B = c_f v|v|$ where c_f is a friction factor, and A_H is the horizontal eddy viscosity (cm²/s).

A vertically-integrated transport equation for the suspended sediment concentration C can be written as

$$\frac{\partial}{\partial t} (hC) + \frac{\partial}{\partial x} (UC) + \frac{\partial}{\partial y} (VC) = b D_H \left(\frac{\partial^2 C}{\partial x^2} + \frac{\partial^2 C}{\partial y^2} \right) + q_s \quad (7)$$

where D_H is the horizontal eddy diffusivity and q_s is the sediment flux at the sediment-water interface. The above equation is valid for each component of the sediment.

A volume integral method was used to derive difference equations which are second-order accurate, explicit, two-time level, and locally conservative. By this procedure, equations which are valid at boundaries as well as in the interior can be readily derived.

A unique feature of the present model is that it can successfully treat open boundary conditions. Procedures formulated by previous authors (see, for example, Kreiss, 1966; Pearson, 1974; Orlanski, 1976; Chan, 1977; Engquist and Majda, 1977) to treat this problem have often worked reasonably well when only outward propagating waves with a well-defined phase velocity

were present. In other cases, the results have not been entirely satisfactory. The procedures have been difficult to generalize when prescribed incoming disturbances were present.

In the present model, a quite general procedure developed by us (Lick et al., 1986, 1987) has been used to successfully treat this problem. The basic idea is to separate the disturbance at the open boundary into outgoing and incoming waves. The incoming waves or disturbances are specified quantities due to known currents, tides, or storm surges. The outgoing waves are due to disturbances generated within the region of interest and need to be determined as part of the problem. By means of the volume integral method, separate difference equations for each set of outgoing or incoming waves can be derived. The resulting difference equations are second-order accurate and explicit. By this means, the propagation of outgoing waves in the presence of specified incoming waves can be modeled with negligible reflection or distortion. The major assumption for the algorithms to be valid is that outgoing waves can be defined, an assumption equivalent to the most general statement of Sommerfeld's radiation condition.

Applications

Results of calculations for three different cases are presented here: (1) the Raisin River, (2) a river flowing into a lake or ocean with a cross-flow, and (3) the time-dependent flow in a simple estuary as affected by tidal currents. The main purpose is to quantitatively understand the resuspension, deposition, and transport of fine-grained sediments in various situations. A secondary purpose is to demonstrate the treatment of open boundary conditions for this type of problem. In all cases, the flow was treated as time-dependent. However, for the first two cases, only steady-state flows

will be described here while, in the third case, only the periodic flow will be described.

Raisin River

The Raisin River is a small polluted stream with relatively high sediment concentrations that flows into the Western Basin of Lake Erie. The bottom topography and computational grid ($\Delta x = \Delta y = 25$ m) are shown in Figure 1. The inflow channel is relatively shallow with a maximum depth of 2 m while the exit channel is dredged to a depth of 5 to 6 m in the center. The turning basin (the wider part of the river) is also dredged periodically and has a depth of 5 to 6 m in the center. Two flow rates were considered corresponding to typical observed low and high flows. These were a low flow with a velocity of 15 cm/s at the inlet and a high flow with a velocity of 45 cm/s at the inlet. The sediment concentration at the inlet was assumed to be 10^{-4} gm/cm³ (100 mg/l) in both cases. For simplicity, a single sediment particle diameter of 10 μ m with a settling speed of 10^{-2} cm/s was assumed. The initial structure of the sediment bed was as follows: top layer, $m = 0.05$ gm/cm², $t_D = 1$ day; second layer, $m = 0.10$ gm/cm², $t_D = 2$ days; third layer, $m = 3.00$ gm/cm², $t_D = 4$ days. Here m is the mass/area and t_D is the time after deposition. Additional parameters used in the calculation were: $A_H = D_H = 2.5 \times 10^4$ cm²/s, $c_f = 0.002$, $a_o = 0.0075$, and $\tau_o = 1$ dyne/cm². The values of the last two parameters are based on laboratory experiments with sediments from the Raisin (MacIntyre et al., 1986).

The calculated currents for the high flow rate are shown in Fig. 2. It can be seen that the currents are relatively high in the straight incoming channel, are low in the turning basin, and are relatively high in the part of the narrow curved section of the channel where the water is relatively shallow.

For the high flow case, the change in the thickness of the sediment bed after 12 hours is shown in Fig. 3. It can be seen that net erosion has occurred where the currents were high (the incoming channel and the lower part of the narrow curved section of the channel) while net deposition has occurred in the rest of the river, especially in the turning basin. From the details of the calculation, it can be shown that, in the erosional areas, the net resuspension is now zero. Resuspension is still occurring but is only due to sediments which have only recently been deposited and hence can be readily resuspended. At the low flow rate, the bottom stress is below critical everywhere and net deposition occurs throughout the river.

The above description is in qualitative agreement with observations of erosional and depositional areas and with estimates of the deposition rates obtained from dredging of approximately 1 m/yr in the turning basin.

River Flowing into a Lake with a Cross-Flow

An important and relatively common sediment transport problem is that associated with a river flowing into a lake or ocean in which there is a cross-flow present. It is assumed here that the river and the lake have a constant depth of 5 m while the river width is 400 m. Calculations with three flow conditions were made: (1) a river velocity of 20 cm/s and a cross-flow (left to right, see Fig. 4) of 5 cm/s; (2) a river velocity of 40 cm/s and a cross-flow of 5 cm/s; and (3) a river velocity of 40 cm/s and a cross-flow of 10 cm/s. Other parameters were: $A_H = D_H = 5.0 \times 10^4 \text{ cm}^2/\text{s}$, $c_f = 0.002$, $a_o = .0075$ and $\tau_o = 0.5 \text{ dynes/cm}^2$. The critical stress τ_o corresponds to a current of about 16 cm/s.

The calculated velocities for the third case are shown in Fig. 4. Although the cross-flow is weak, it has a significant effect on the flow field and sweeps the river plume to the right. It can be seen that a weak

vortex with velocities of 1 cm or less has formed downstream of the river mouth. The open boundary condition works well with the outgoing flow and disturbances passing through the boundary with negligible reflection or distortion.

Sediments of three different sizes (diameters of 1, 3, and 10 μm) were assumed to be present simultaneously. In the river, the concentration of each sediment group was assumed to be 100 mg/ℓ . The initial structure of the sediment bed was the same as that for the Raisin River.

The changes in the thickness of the bottom sediments after 24 hours for the three cases are shown in Figs. 5(a), (b), and (c). For all three cases, it can be seen that erosion has occurred in the river channel and in an area near the river mouth. This latter area increases rapidly as the flow velocities increase. Accumulation of sediment occurs downstream of the eroded area with a very rapid increase in sediment thickness near the river mouth at the downstream edge of the eroded area, a common observed feature in flows of this type. This is due to the fact that strong currents in the river plume erode the sediments near the mouth of the river while very weak currents due to the vortex are present downstream of the mouth, do not erode the sediments, but do transport the suspended sediments toward the plume. The typical sand bar downstream of the river plume is evident in all three figures and is due almost entirely to the deposition of the larger particles with diameters of 10 μm .

The Flow in a Simple Estuary

The time-dependent flow and sediment transport in an estuary with simple geometry (see Fig. 6) is considered here. The estuary is rectangular, 20 km long and 16 km wide. The river flowing into the estuary is 3 km wide while the mouth of the estuary is 7 km wide. The water depth is uniformly 20 m.

The initial structure of the sediment bed was: first layer, $m = 0.4 \text{ gm/cm}^2$, $t_D = 1 \text{ day}$; second layer, $m = 0.4 \text{ gm/cm}^2$, $t_D = 2 \text{ days}$; third layer, $m = 3.0 \text{ gm/cm}^2$, $t_D = 3 \text{ days}$. Other parameters were specified as: $\tau_o = 2 \text{ dynes/cm}^2$, $a_o = 7.5 \times 10^{-3}$, $c_f = 0.002$, $A_H = 5 \times 10^5 \text{ cm}^2/\text{s}$, and $D_H = 5 \times 10^6 \text{ cm}^2/\text{s}$.

The boundaries at both A and B (see Fig. 6) were treated as open boundaries. The undisturbed inflow velocity of the river at A was set at 20 cm/s. This is modified by time-dependent tidal effects which cause disturbances to propagate from the estuary into the river in an upstream direction. The tidal forcing at B, the mouth of the estuary, was assumed to be generated by a time-varying surface elevation given by

$$\eta = A_1 \cos(\omega_1 t - \phi_1) + A_2 \cos(\omega_2 t - \phi_2) \quad (3)$$

where $A_1 = 100 \text{ cm}$, $A_2 = 60 \text{ cm}$, $\omega_1 = 2.25 \times 10^{-5} \text{ Hz}$, $\omega_2 = 2.51 \times 10^{-5} \text{ Hz}$, $\phi_1 = 235^\circ$, and $\phi_2 = 251^\circ$. This describes the incoming wave at B. The change in the total surface elevation is due to the sum of this incoming wave and the outgoing waves caused by disturbances within the estuary.

The hydrodynamic calculation was continued for 48 hours, or about four tidal cycles. After an initial transient, the solution became essentially periodic with time. This periodic flow field at two hours after ebb tide is shown in Fig. 6. The maximum velocity in the river is now about 30 cm/s. The maximum velocities in the system occur near the mouth of the estuary and are about 120 cm/s. After this time, currents throughout the system generally decrease with time until about two hours after flood tide (8 hours after ebb tide). At this time, the currents are generally less than 10 cm/s in the estuary. The strongest currents are in the river (20 cm/s) where the currents are now reversed with the flow going upstream at A. The flow at B

is into the estuary as expected but is much weaker than the flow at ebb tide. The open boundary condition works well and allows disturbances to propagate up the river as well as out of the mouth of the estuary without noticeable reflections or distortions.

The suspended sediment concentration throughout the estuary was assumed to be zero at the beginning of the calculation while the suspended sediment concentration at A in the river was maintained constant at 100 mg/l independent of time. Separate calculations were made for particles with diameters of 3, 10, and 30 μm . The change in the thickness of the bottom sediment for the 10 μm particles after 48 hours is shown in Fig. 7. Net erosion has occurred near the mouth of the estuary (maximum erosion is 2.2 gm/cm²) while only a small net deposition has occurred in the rest of the estuary.

Near the river mouth, deposition is high because of the high suspended sediment concentration but resuspension is also high because of the strong currents there. The result is little net deposition. Near the mouth of the estuary, the currents are strong and the resuspension of the first two layers of the bottom sediments is rapid after which the resuspension rate decreases rapidly. After this, any deposited sediments are then immediately resuspended. After the first few hours that it takes for the resuspension of the first two layers to occur, the depth of erosion is essentially constant. In the rest of the estuary, deposition and resuspension are in a dynamic equilibrium leading to a zero net deposition.

For 3 and 30 μm particles, the patterns of erosion near the mouth of the estuary are much the same as those for the 10 μm particles. However, the deposition near the river mouth is quite different; the 30 μm particles settle out rapidly near the river mouth while the 3 μm particles hardly settle at all and are transported into and then out of the estuary.

Summary and Conclusions

Recent laboratory and field data on the resuspension and deposition of fine-grained sediments has been used to develop a physically realistic description and numerical model of the sediment bed and the flux of sediments from this bed. From this, changes in the sediment bed with time due to resuspension, deposition, and compaction can be determined.

This information has been incorporated into a hydrodynamic and sediment transport model. In this model, the sediment bed is approximated by layers in each of which the properties are independent of depth but may vary with time. The model can also treat conditions at open boundaries accurately and realistically. An interesting demonstration of this was the treatment of open boundaries in an estuary when the flow was time-dependent due to tidal currents.

The model has been applied to several typical problems concerned with the resuspension, deposition, and transport of fine-grained sediments. Erosional and deposition features that are commonly observed in these flows were reproduced. By means of the model, the parameters on which these features depend can be accurately determined. Steady and time-dependent flows can be analyzed.

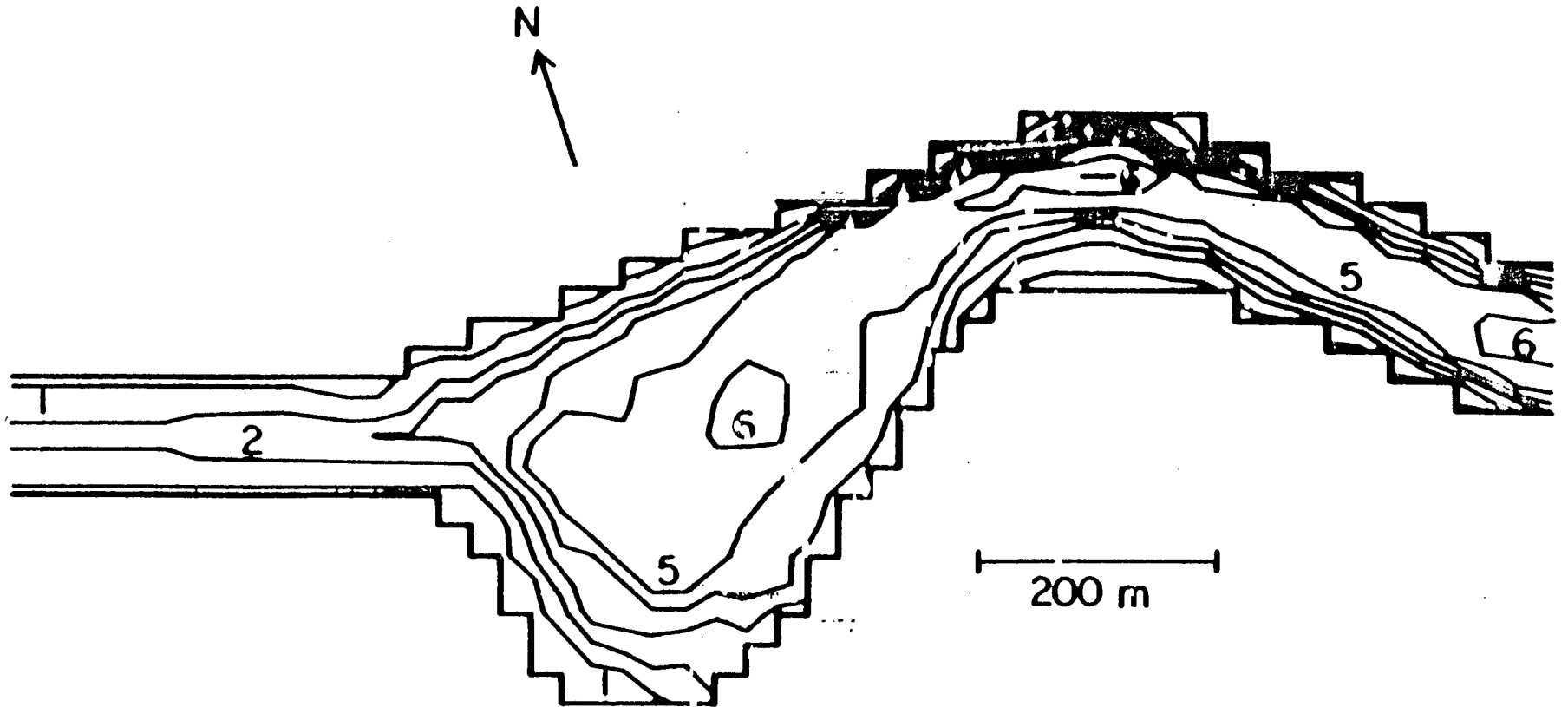


Fig. 1. Bottom topography for the Raisin River. Depth in meters.

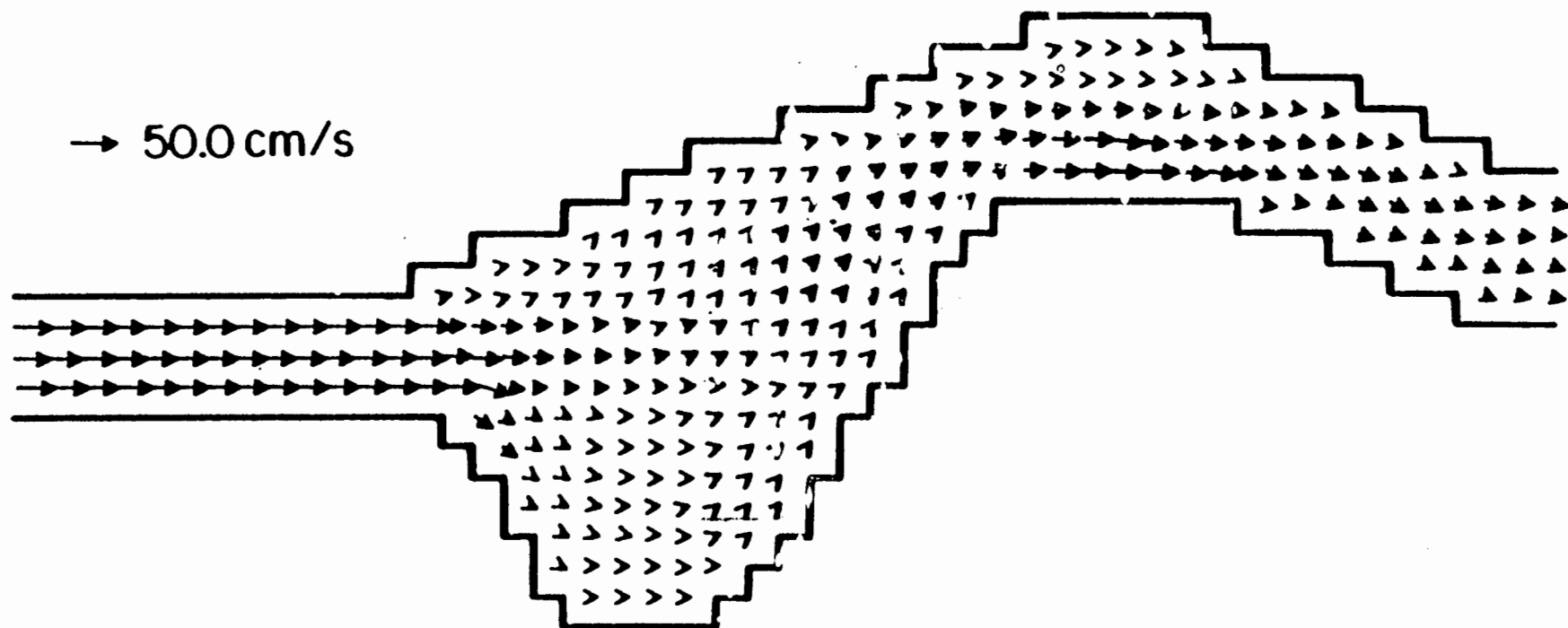


Fig. 2. Currents in Raisin River High flow rate.

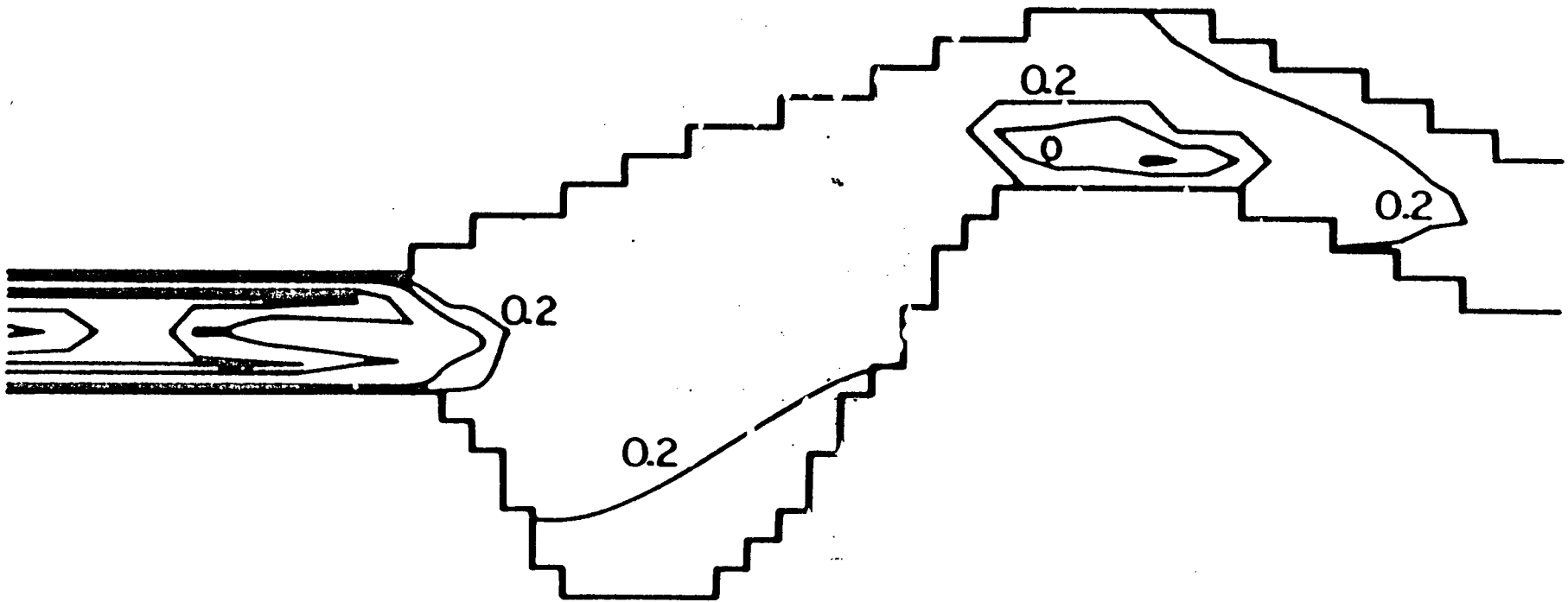


Fig. 3. Changes in the thickness of the bottom sediments (gm/cm^2) in the Raisin River after 12 hours.

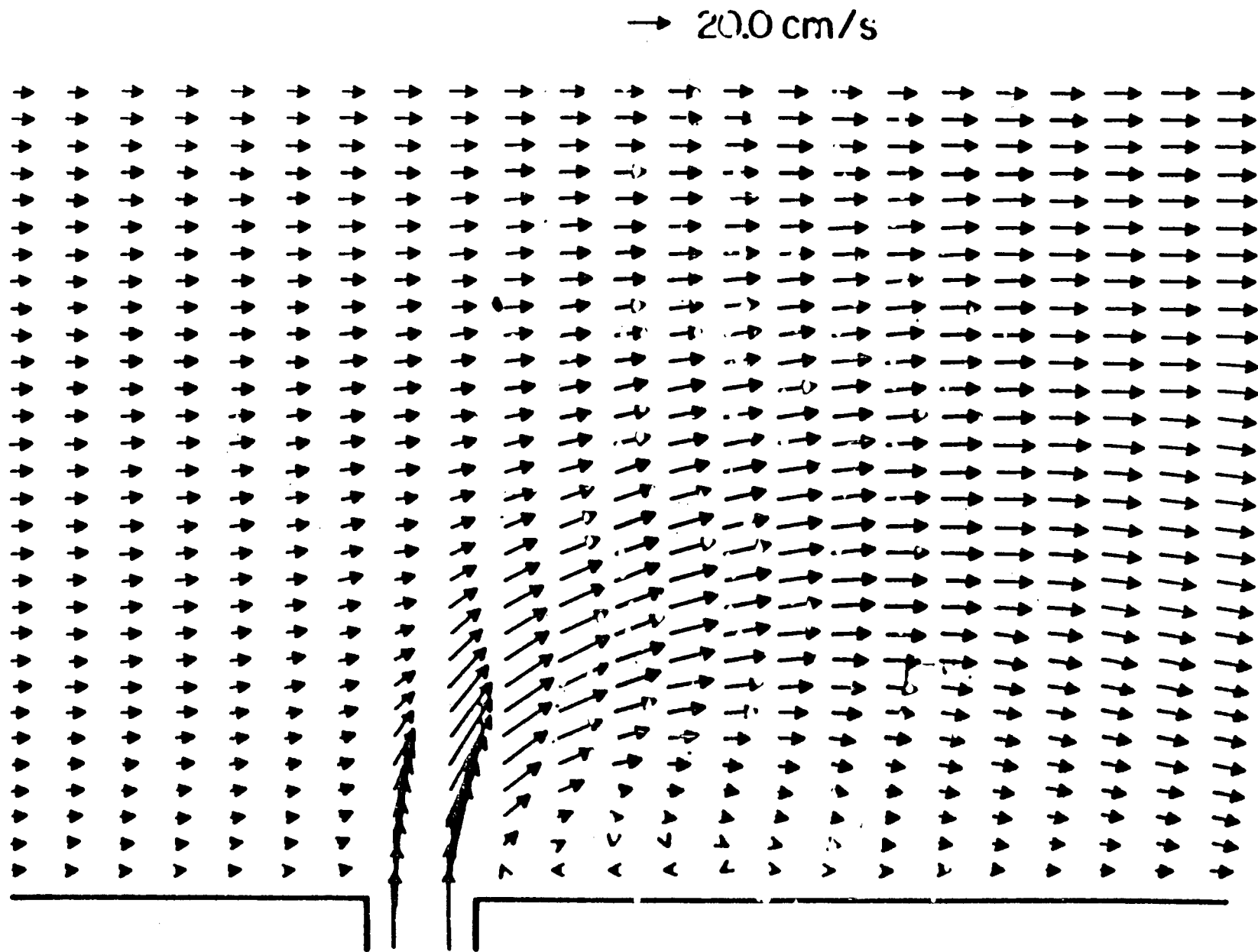


Fig. 4. Flow field when the river flow is 40 cm/s and the cross-flow is 10 cm/s.

For clarity, only every second column of velocity vectors is shown.

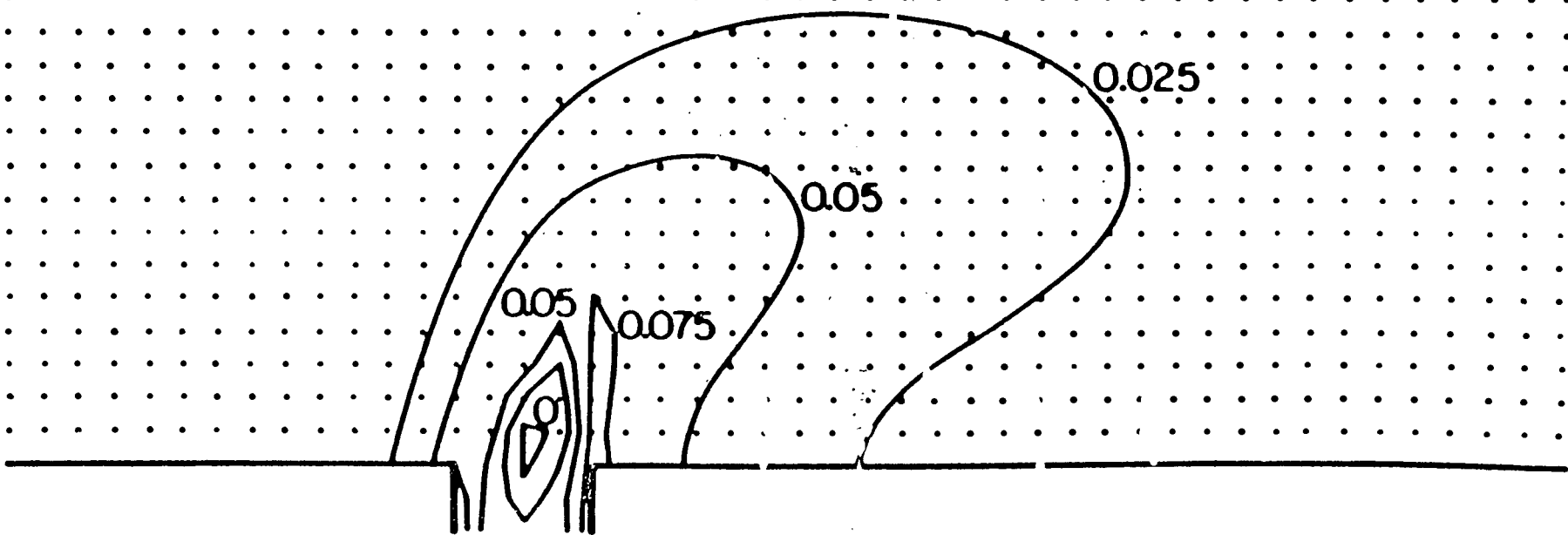


Fig. 5a. Changes in the thickness of the bottom sediments (gm/cm^2) after 24 hours.
River flow is 20 cm/s and the cross-flow is 5 cm/s

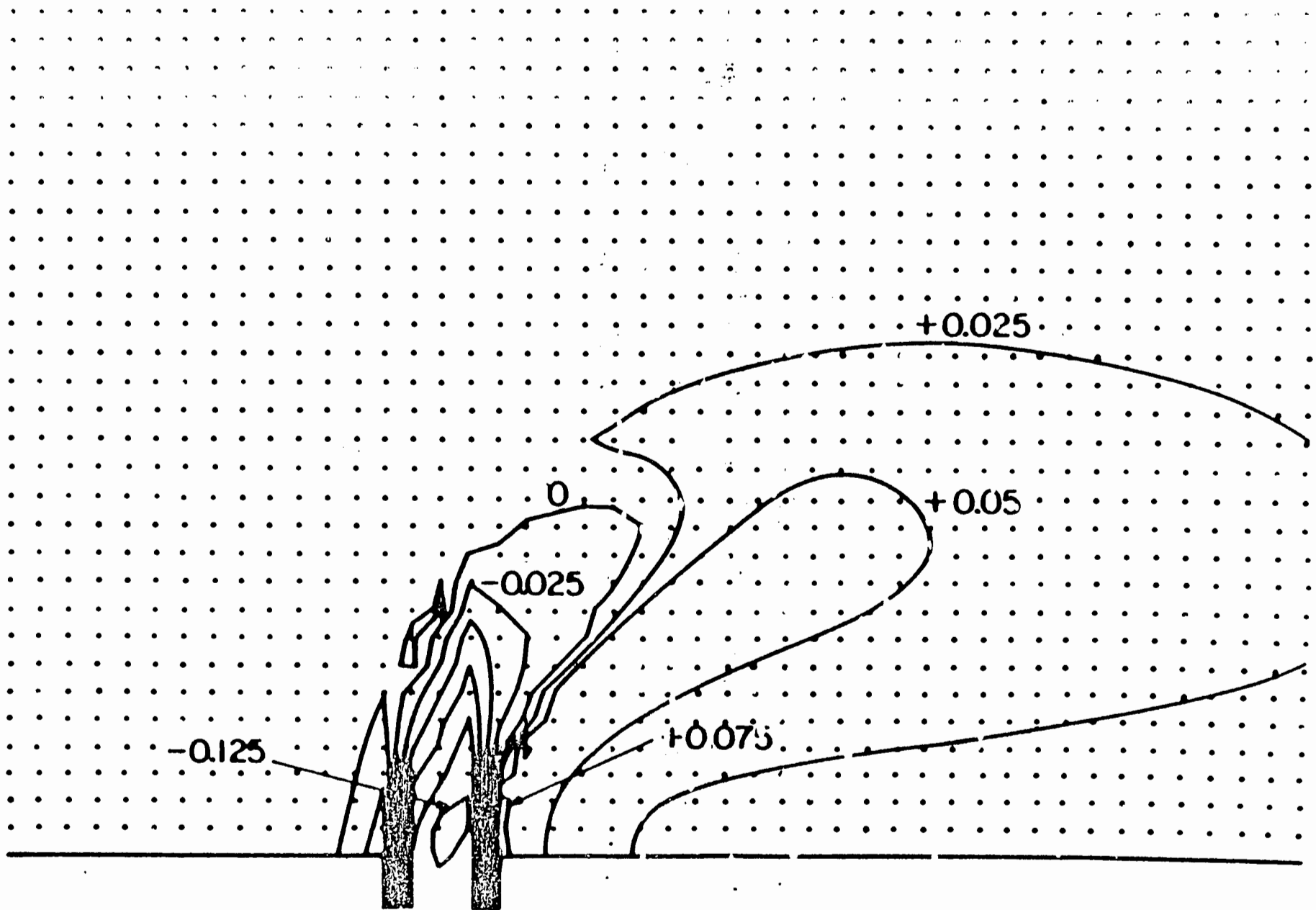


Fig. 5b. Changes in the thickness of the bottom sediments (gm/cm²) after 24 hours.

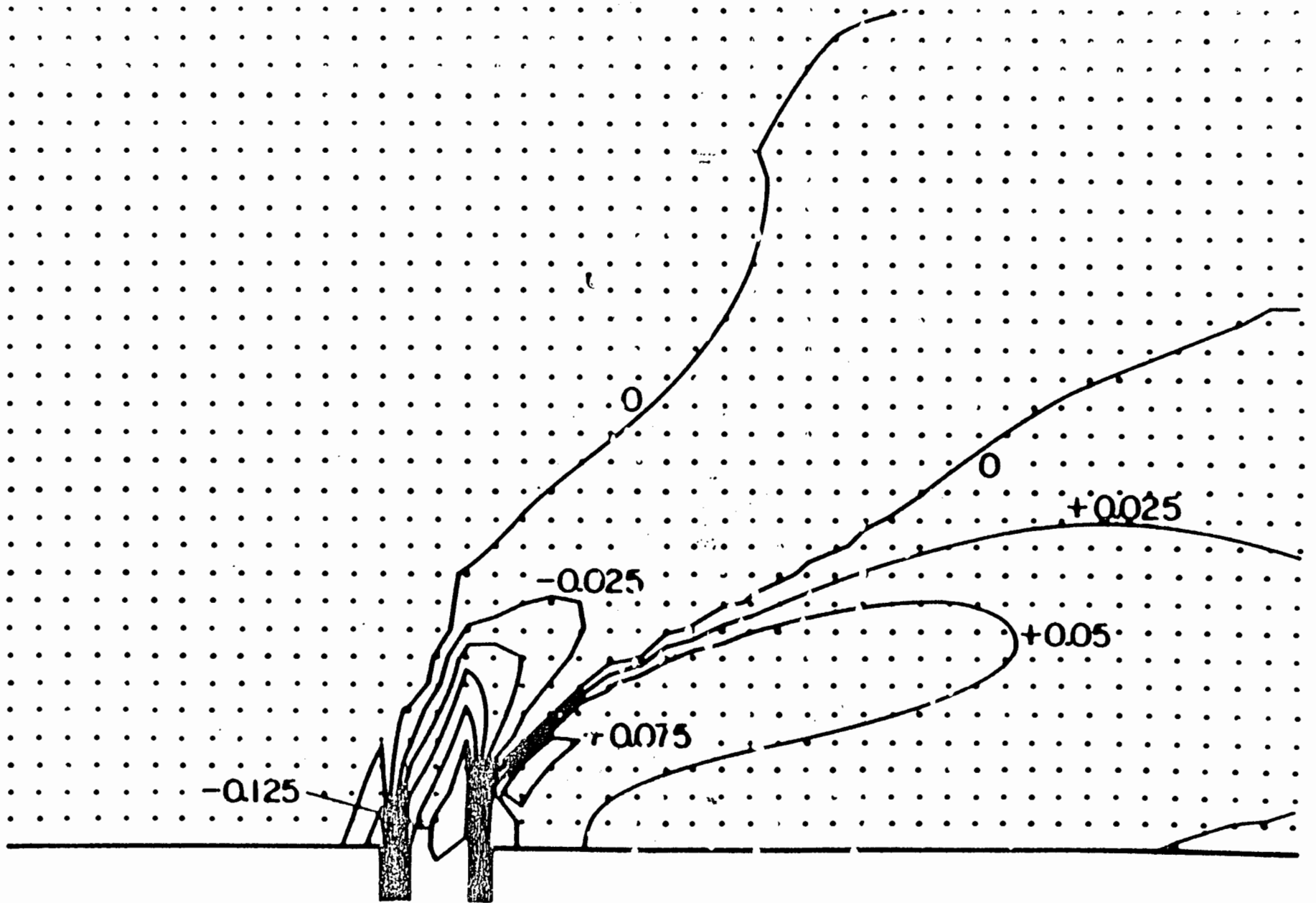


Fig. 5c. Changes in the thickness of the bottom sediments (gm/cm^2) after 24 hours.
River flow is 40 cm/s and the cross-flow is 10 cm/s.

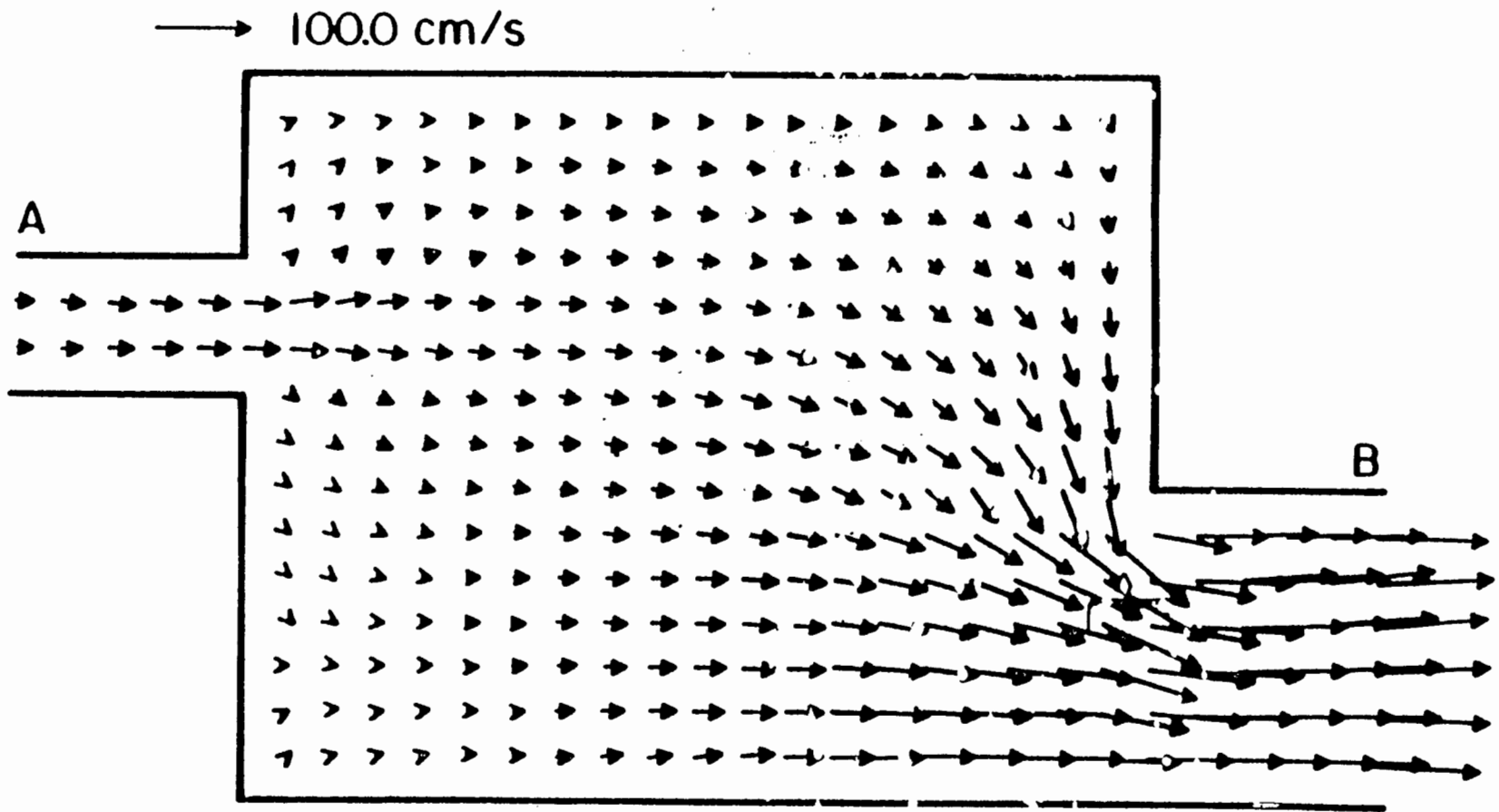


Fig. 6. Currents in the estuary at two hours after ebb tide.

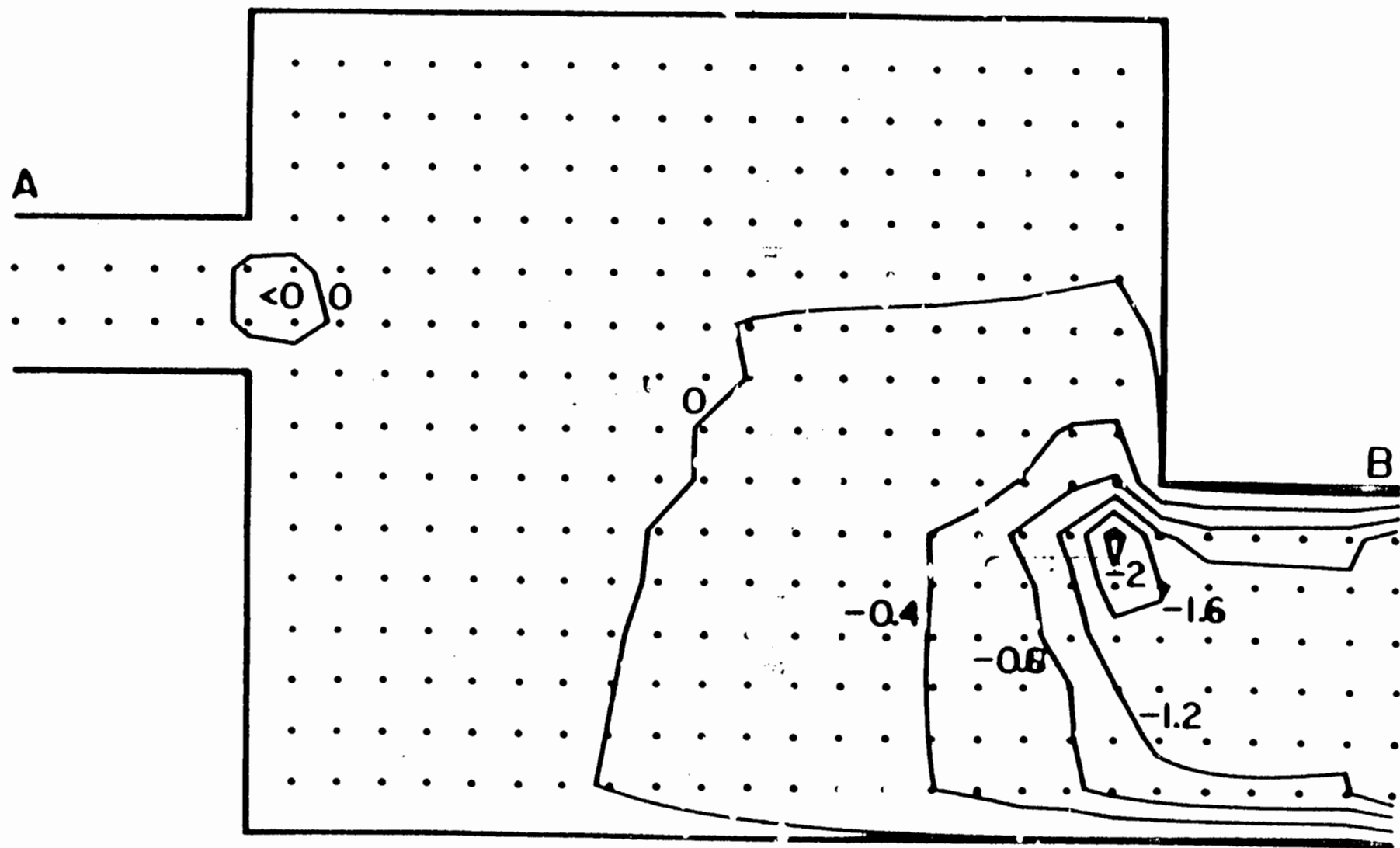


Fig. 7. Changes in the thickness of the bottom sediments (gm/cm³) for the 10 μ m particles after 48 hours.

A SEDIMENT RESUSPENSION STUDY IN THE DETROIT RIVER

Many laboratory experiments have been carried out to determine sediment resuspension as a function of its governing parameters: applied shear stress, time of deposition, particle size distribution, water chemistry, and benthic organisms (Partheniades, 1965; Mehta and Partheniades, 1975; Fukuda and Lick, 1980; Lee et al., 1981; MacIntyre et al., 1986; Tsai and Lick, 1986). However, the properties of sediments in situ are not well known and they also vary with time and location. Hence, the application of laboratory results to the field is not well developed.

For these reasons, a portable device for measuring the resuspension of undisturbed sediments has been developed (Tsai and Lick, 1986). It has been shown that this device can be used in the laboratory for quick and reasonably accurate measurements of resuspension. It can also be used on board ship for rapid surveys of the resuspension of relatively undisturbed sediments throughout an aquatic system.

The shaker consists of a cylindrical chamber inside of which a horizontal grid oscillates vertically (Figure 8). The chamber contains a layer of sediment whose properties are to be studied and a layer of water overlying the sediment. Turbulence created by the grid oscillating in the overlying water causes the sediment resuspension. The turbulence and hence the amount of sediment resuspended is proportional to the frequency of the grid oscillation.

At the beginning of a shaker resuspension test, the sediment concentration in the overlying water is relatively low. After the start of the test, the sediment concentration in the water layer increases rapidly in the first 5 minutes and then more slowly. The sediment concentration usually reaches a

steady state about 10 minutes after the start of the test. It has been shown that for cohesive sediments the amount of sediment that can be resuspended by a given applied shear stress is finite (Massion, 1982; MacIntyre et al., 1986; Tsai and Lick, 1986) and that the steady state concentration obtained in the shaker is a reasonable estimate of that amount (Tsai and Lick, 1987).

The following section gives a description of the shaker and the modifications of the shaker chamber required for this study. The locations and the sediment samples obtained in this study are then described. Finally, the results of the resuspension tests are presented.

Shaker

The shaker grid is a 0.6 cm thick plexiglas disc which has a diameter of 11 cm and which is perforated with holes 1.2 cm in diameter. The distance between the centers of two neighboring holes is 1.5 cm.

The grid is powered by a variable speed motor. Between the motor and the grid is a drive disc fixed to the motor shaft, a linkage bar attached to the disc, and a drive rod fastened to the linkage bar (Figure 1). The bar is set 1.27 cm off the center of the disc to create an up and down motion of 2.54 cm. The shaker chamber is made of cast acrylic tubing which has an outside diameter of 12.7 cm and an inside diameter of 11.7 cm. The chamber is 27.9 cm high and has a sampling port for measurement of sediment concentration.

The shaker was calibrated by comparison of results with those in an annular flume. The equivalent shear stresses created by the oscillating grid were determined by comparisons of sediment concentrations in the shaker and in the flume. Exactly the same type of sediments were deposited into both devices and the sediments were then allowed to settle for the same length of

time. During the calibration, the depth of the overlying water inside the shaker core was adjusted to be 12.7 cm, i.e., the volume of the overlying water was 1.36 liters. Also the lower surface of the grid was adjusted to be 5.08 cm above the sediment surface, i.e., the grid oscillates between 5.08 and 7.62 cm above the interface. By running the shaker at given speeds and the flume at known bottom shear stresses, the concentrations of resuspended sediments in both devices were compared, and the equivalent shear stresses of the shaker were thus determined. Shown in Figure 9 is the relationship between the equivalent shear stress and the period of grid oscillation. As can be seen from the figure, three tests were carried out and the equivalent shear stresses produced by the shaker are reproducible. The equivalent shear stress created by the shaker is 2.5 dynes/cm² when the grid oscillating period is 0.14 second. The stress increases linearly (on a logarithmic scale) to 5 dynes/cm² as the period decreases to 0.08 second.

A field trial of the shaker was carried out in Lake St. Clair. For the field tests, the cylindrical chamber of the shaker was modified and consisted of three parts: a cylindrical tube, a bottom disk, and a top plate. The sediment samples were obtained by a diver as follows. The diver first gently pushes the tube into the sediment. The bottom disk is then forced into the sediment from the side of the tube and slid to the location of the tube. Finally, the top plate is placed on top of the tube to prevent any disturbance to the sediment-water interface as the sediment core is brought up to the ship. In this field trial, it was found that with this method, relatively undisturbed sediment samples can be obtained. By this procedure, differences in properties of sediments from different locations can readily be determined.

In highly contaminated areas, such as some areas in the Detroit River, the above sediment coring method was unsatisfactory. In this case, the samples have to be obtained without a diver. Therefore, the shaker was again modified. The procedure for obtaining sediment cores was to lower the shaker to the bottom and push it into the bottom sediments with a pole. The sediment sample inside the tube was retained by the cohesion between sediment particles and by the friction between sediments and tube wall while it is being pulled up. The length of the cylindrical tube was increased to 30.5 cm to accommodate a longer sediment sample. The top plate of the tube was replaced by a chamber cap. The cap was made of a tubing whose inside diameter coincides with the outside diameter of the cylindrical tube. Inside the cap, an O ring was installed to prevent any leaks when the cap is mounted on top of the tube. A flat plate was glued on top of the chamber cap. The plate was drilled with a hole (5 cm) on top of which a rubber valve was mounted.

To collect sediment samples, the chamber cap is first mounted on the cylindrical tube and a ring type of clamp is clamped on the joint. The tube is then secured onto a pole by the use of two ring type clamps. As the tube is lowered into the water, the majority of the air inside the tube escapes through the rubber valve. It is important to eliminate the remaining air bubbles. This was done by shaking the tube a few times while it was immersed in the water. After this, the tube was lowered onto the bottom and forced into the sediment layer for about 9 to 15 cm. Finally, the tube was slowly pulled up. While the sediment core is being pulled up, the cohesion between sediments keeps the sediments together. The friction between the sediments and the tube wall prevents the sediments from falling out. Before the core is pulled out of the water surface, the bottom disk is carefully forced into the bottom of the chamber to hold the sediments in place.

The success of this sediment coring technique mainly depends on the type of sediment. The method works best for cohesive sediment. If the sediment consists of only loose sand, there is generally not enough cohesion and friction to hold the sediment in place. However, in the area of the present study, the sediment often contained some cohesive layers or organic materials that prevented the sediments from falling out. Hence, this technique worked successfully.

Results

Sediments were collected from eight stations in the Detroit River (Figure 10). These included four master stations, 30, 34, 53, and 83, and four sub-stations, 42, 46, 53A, 53B. Sediments at the first three master stations were known to contain high concentrations of contaminants while station 83 was a reference site where the sediments were relatively free from contamination. Station 30 is located to the south of the toll bridge between Detroit and Grosse Ile and at the western bank of the river downstream from Monagan Creek. At this station, the ship was tied to the pilings on the breakwall. Sediments from this station were very oily and they had a strong petroleum odor. These sediments also contained pockets of gas, possibly carbon dioxide, and the gas was spontaneously released to the water column. From qualitative observations, the sediments had a brownish color and consisted of silt, clay, and sand.

Station 34 is located in a small lagoon, called Black Lagoon, on the western bank of the Detroit River. The sediments from this station were also very oily, with a strong petroleum odor, and with gas pockets. A unique feature of these sediments was that they consisted mostly of dark coal-like particles and some gray colloidal particles. When these sediments were

disturbed, the dark particles settled quickly while the colloidal ones remained in suspension for a long period of time.

Station 53 is located south of Gibraltar and at the outlets of Brownstown Creek and Frank and Poet Drain. The sediments obtained from this station were mostly sand with a small quantity of silt and coal-like particles. Mats of algae were also present on top of the sediments.

The last master station is station 83 which is near the western bank of Fighting Island. The sediments here were mainly very compacted clay and silt. They had a gray color and weed growth.

The locations of stations 53A and 53B were close to station 53. The sediments from these first two stations appeared similar to those found in the latter station. Station 42 is in the Monsanto Lagoon which is just south of the Monsanto Chemical Company. This station's sediments were oily and with a petroleum odor, but to a lesser degree than those found in stations 30 and 34. The sediments contained silt and clay with the silt layer overlying the clay layer. They also had a thin growth of weed on the surface. The location of station 46 is just to the north of the Humbug Marina. The sediments were sandy and had organic debris and algal mats overlying the sediment layer. For easy reference, the qualitative observations of the sediments from each station are summarized in Table 1.

At each station, 2 to 5 sediment cores were obtained and they were subjected to a shear stress ranging from 2.5 to 5 dynes/cm². Before starting the shaker experiment, the concentration of the suspended solid in the overlying water was measured. This was done by withdrawing a quantity of water (about 50 ml) and passing it through a filter. By drying and weighing the filter, the suspended solid concentration was determined. Each core was

tested for 25 to 30 minutes and the overlying water sediment concentration was sampled every 5 minutes. In general, the sediment concentration increased rapidly in the first 5 minutes and reached a steady-state in 10 minutes. After this, the sediment concentration often decreased slowly with time. This is due to the compaction of the sediment sample by the oscillating pressure created by the grid. Shown in Figure 11 are the typical time histories of the sediment concentration in the shaker. Figure 11(a) shows the results from station 30. At this station, 2 cores were tested with an equivalent shear stress of 2.5 dynes/cm^2 and 3 cores were tested with a stress of 5 dynes/cm^2 . As one can see, the steady-state concentrations for the 2.5 dynes/cm^2 tests were 600 and 500 mg/l, while the steady-state concentrations for the 5 dynes/cm^2 tests were 4000, 6400, and 7000 mg/l. The averaged steady-state sediment concentration is 605 and 5200 mg/l for the 2.5 and 5 dynes/cm^2 test respectively (also see Table 2). The concentration-time plot shown in Figure 11(b) shows the results obtained from station 34. At this station, one core was tested with an equivalent stress of 2.5 dynes/cm^2 , and the steady-state concentration was 1100 mg/l; while two cores were tested with a stress of 5 dynes/cm^2 , and the concentrations were 7000 and 8000 mg/l. From Figure 11, one can see that the results between duplicating tests agree quite well. This is also true for the stations not shown in Figure 11. Some large variations, such as the one from 4000 to 7000 mg/l at station 30, can be attributed to the difference in sediment properties, because sediment properties can change in just a few meters of distance. However, the variations of concentration were all less than a factor of two.

Listed in Table 2 are the steady-state sediment concentration obtained from each station. If multiple cores were tested for the same equivalent stress, the average concentration is tabulated.

Comparison tests were also carried out to see whether there was a difference in sediment resuspension properties between the cores obtained by the pole and by a diver. These tests were carried out at stations 53A, 53B, and 46. The results of this comparison test are shown in Figure 12. At station 53A (Figure 12(a)), 2 cores each were taken by each coring method, and they were tested with stresses with 2.5 and 5 dynes/cm². From the figure, one sees that with a 2.5 dynes/cm² stress both the pole core and the diver core had no entrainment; the concentration was constant with time at 140 mg/l. With a stress of 5 dynes/cm², both the pole core and the diver core had a concentration of 1100 mg at 15 minutes after the start of the tests, indicating good agreement between the two cores. After this time, the pole core's concentration decreased slightly and the test was interrupted by a power failure. On the other hand, the concentration of the diver core increased slightly to 1600 mg/l and remained steady until 15 minutes after the start. After this, the concentration in this core increased to 2500 mg/l. This increase may be caused by a drastic change in the sediment properties at depth in the sediment. After 15 minutes of testing, the sediment was scoured to a layer which was easier to resuspend than the overlying layer. This phenomenon was also seen at station 53B, whose sediment properties were similar to those at station 53A. The test results from station 53B are plotted in Figure 12(b). As can be seen, two diver cores and two pole cores were tested. Among them, three tests showed an increase of sediment concentration by the end of the test. At this station, two diver cores were first obtained and tested. The applied equivalent shear stress was 4 and 5

dynes/cm², and the concentration increased from a quasi-steady value of 500 mg/l to 800 mg/l for the smaller stress, while for the higher stress the concentration was changed from a quasi-steady-state 3000 mg/l to 3800 mg/l. After the tests with the above two cores, two more cores were taken by the pole. At that time, a weather system moved in and the bottom sediments were stirred up. This can be seen from the high initial concentration for the two pole cores, 250 mg/l as opposed to 70 mg/l for the diver cores. Both of these two cores were tested with a stress of 5 dynes/cm². Since some surficial sediments in these two cores were already resuspended, there were less sediments available for resuspension in the shaker. The two pole cores all show lower concentrations than the diver cores.

The last comparison test is shown in Figure 12(c). With a stress of 4 dynes/cm², the concentration from the pole core agreed with that from the pole core, and the steady-state concentration was about 500 mg/l. However, the concentrations for the 5 dynes/cm² tests did not agree as well. The concentration in the pole core did not reach a steady-state in 20 minutes, and the concentration was 1600 mg/l. On the other hand the diver core had a steady-state concentration of 2400 mg/l in 15 minutes. The difference is again due to the difference in sediment properties. It was observed that this diver core tested with 5 dynes/cm² stress had more loose organic material overlying the sediment surface than the other cores from this station. Therefore, this core had a higher concentration.

Summary

The resuspension properties of the bottom sediments in an aquatic system at a given time is important information for predicting sediment and contaminant transport. For predicting sediment transport in the Detroit River a

portable device, called a shaker, was used to measure the resuspension of relatively undisturbed sediments in the river. The sediment samples were obtained either by a diver or by a pole. Samples were obtained from eight stations, and were subjected to equivalent shear stresses ranging from 2.5 to 5 dynes/cm². The results of this field experiment are summarized below.

1. Sediment composition and properties differ significantly from one area to another. In general, the areas around the deep shipping channel have no sediments, except a few sand bars sparsely distributed. Farther away from the channel, more sediment can be found. Along the banks of the river, the sediments were either silty sands with dense weed growth or silts and clays with traces of sands in some relatively stagnant lagoon-like water bodies.

2. Sediment properties may also vary within a few meters in one area.

3. A sediment coring technique was developed so that sediment samples can be obtained without a diver. This technique enables one to test the sediments from areas which are highly contaminated.

4. In general, multiple cores obtained at one station and tested with the same shear stress showed good reproducibility. Variations between duplicates were due to the difference in sediment properties. The variations in sediment concentration, however, were within a factor of two.

5. Comparison tests were carried out for the sediment cores obtained by a diver and the cores obtained by a pole. It was found that there was no significant difference between these two types of sediment cores.

6. The steady-state concentrations obtained with an equivalent shear stress of 2.5 dynes/cm² ranged between 140 and 1100 mg/l. With a stress of 5 dynes/cm², the concentrations were between 2500 and 7000 mg/l.

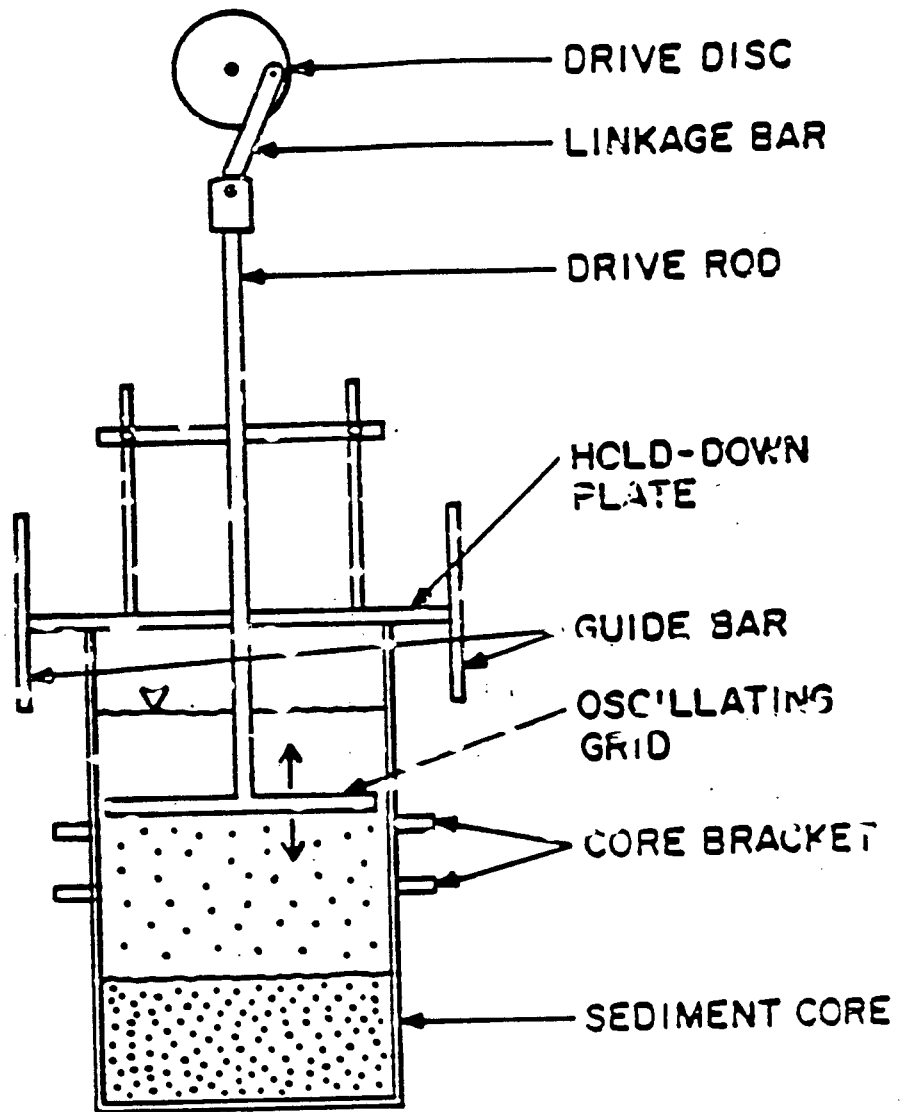


Figure 8. A schematic of the shaker.

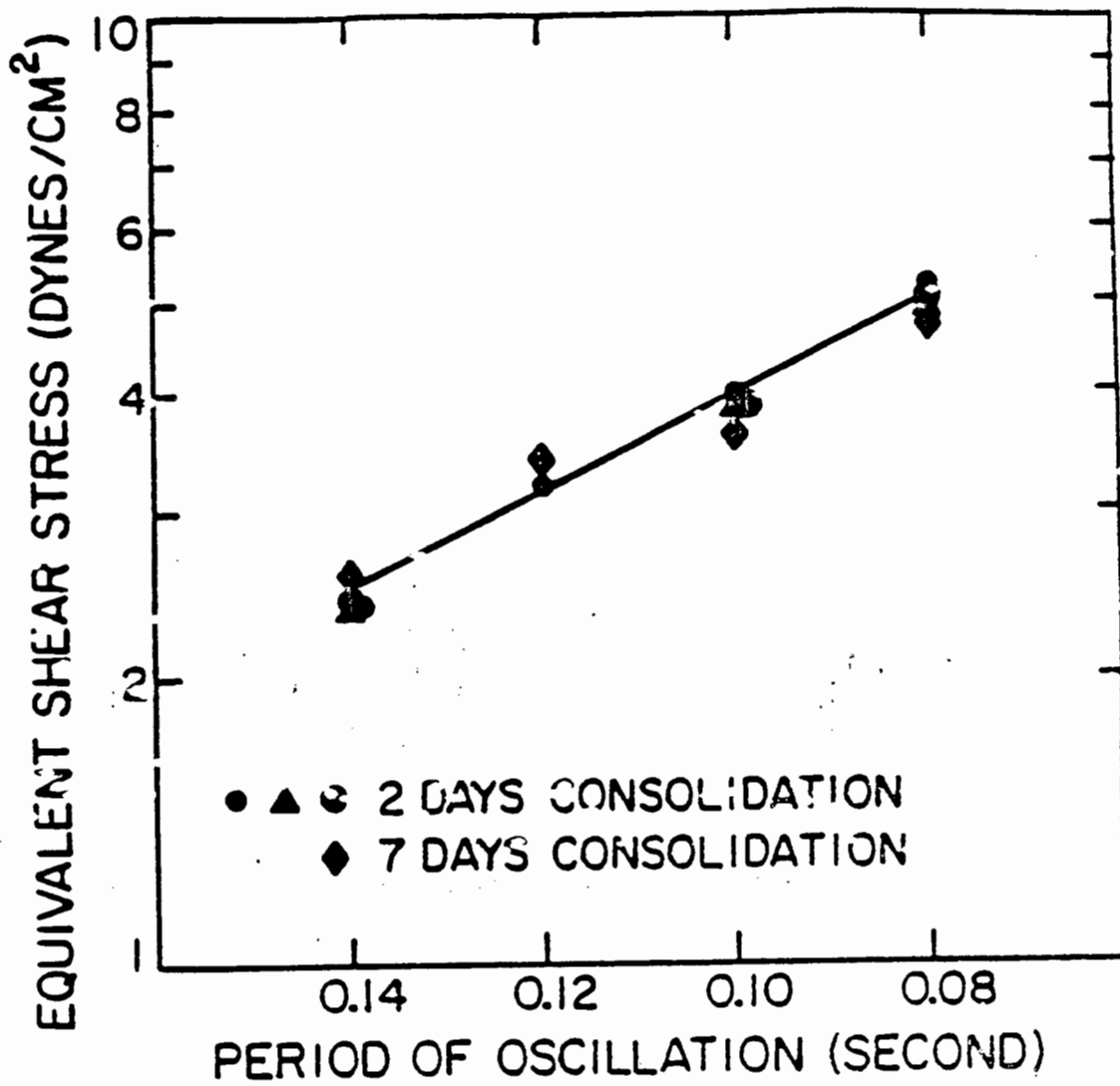


Figure 9. Equivalent shear stresses for the shaker as a function of the period of grid oscillation.

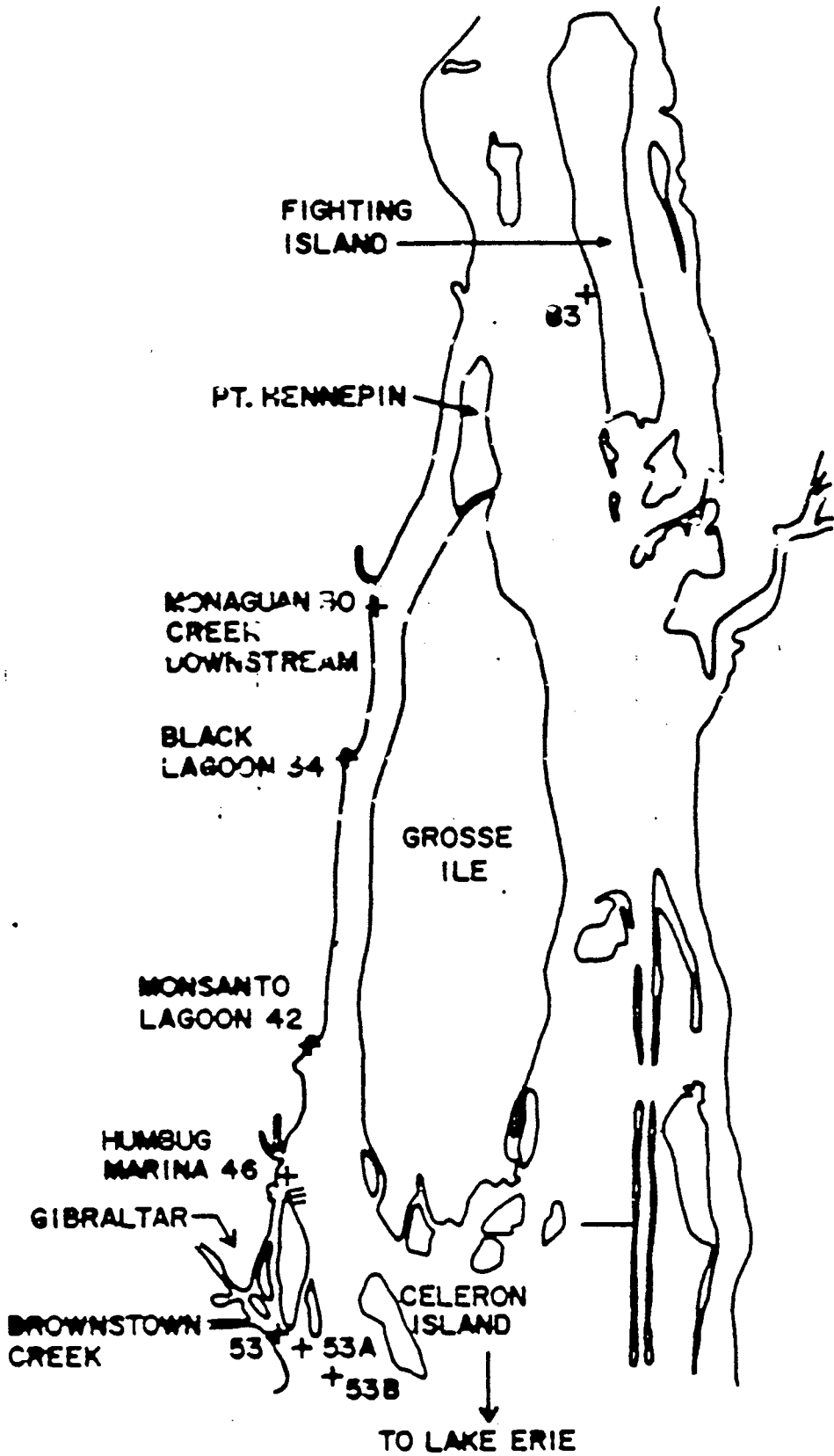


Fig. 10 Study area and sampling stations in the Detroit River.

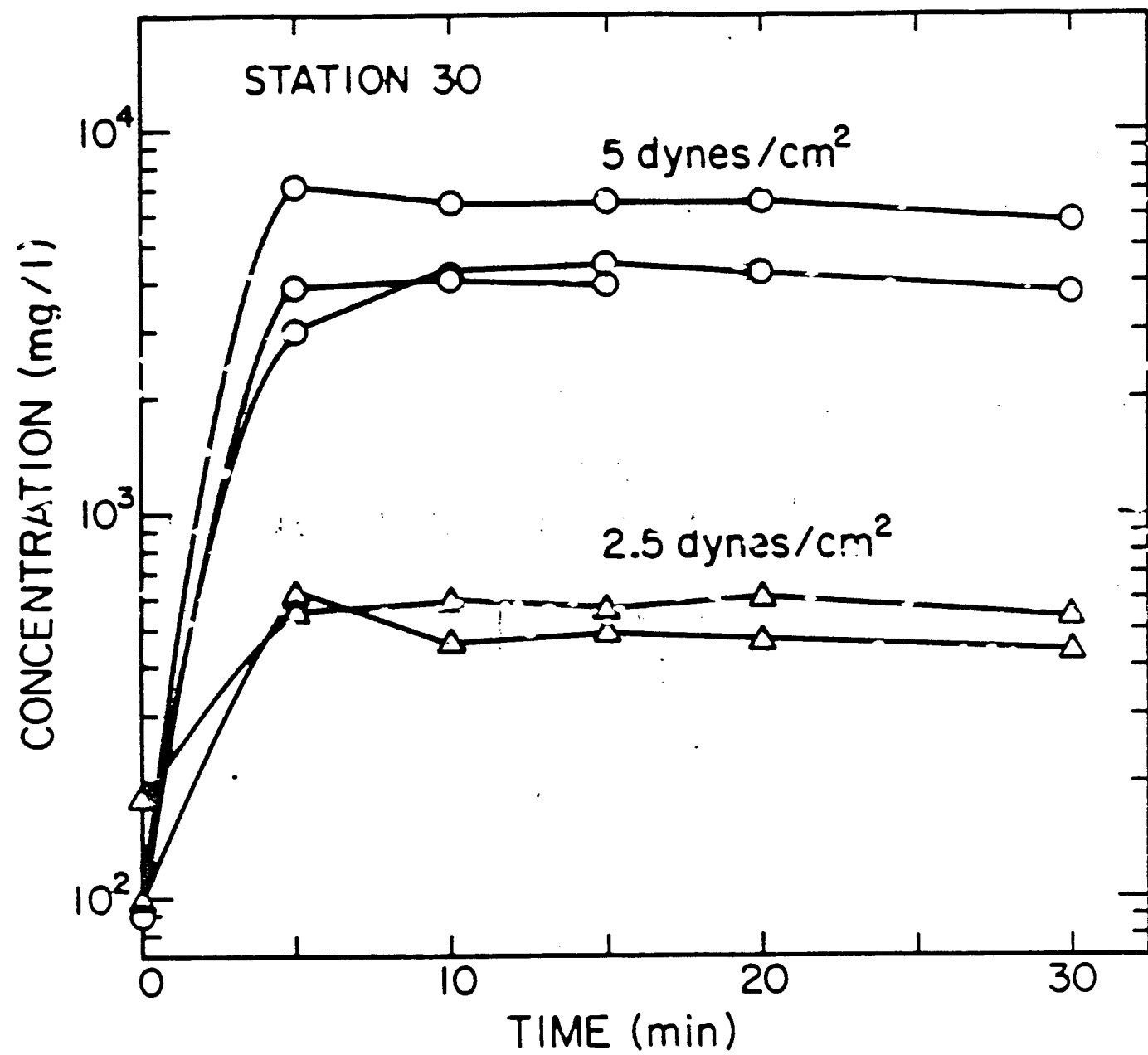


Fig. 11a Typical sediment concentrations in the shaker as a function of time.

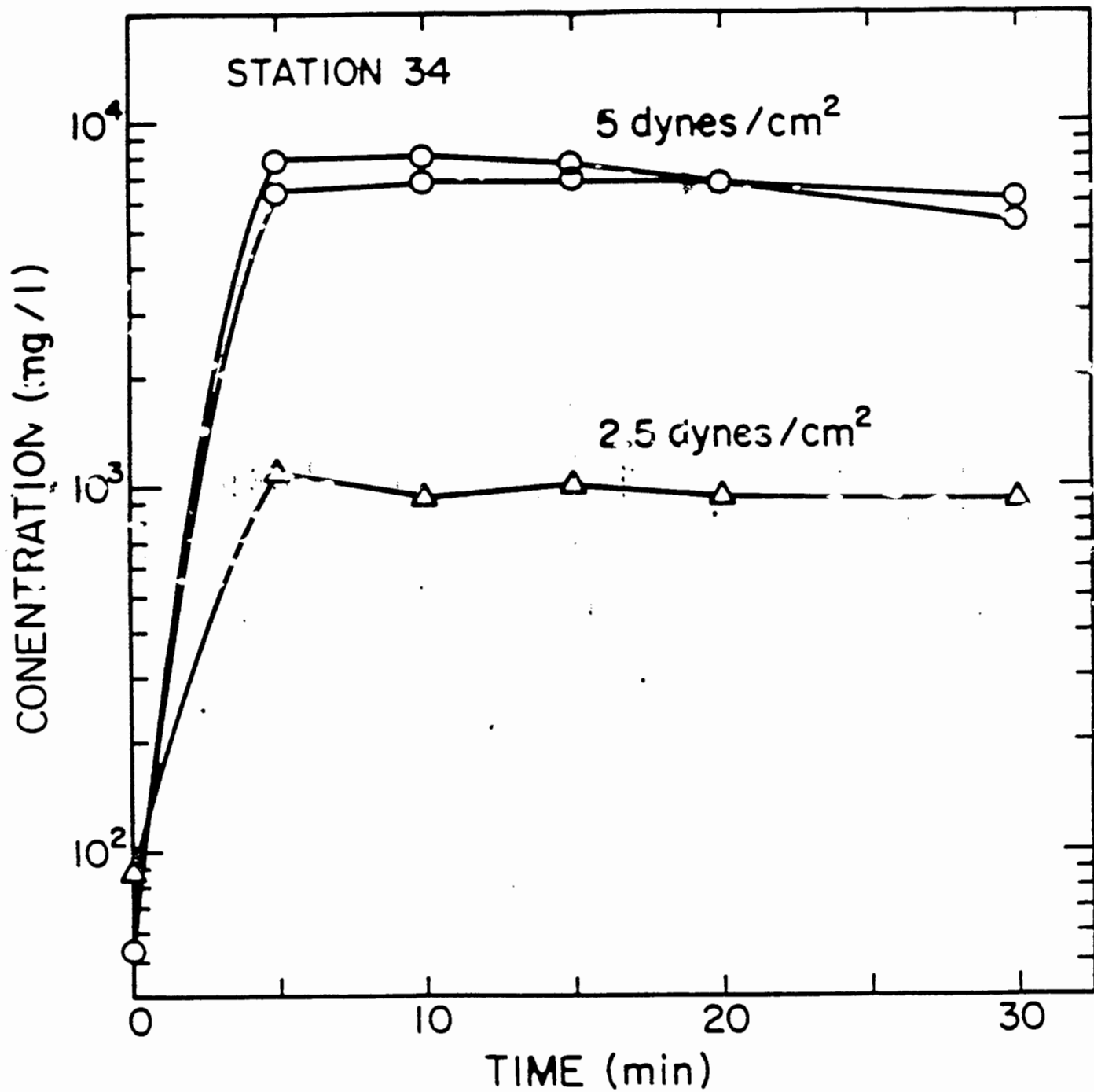


Fig. 11b Typical sediment concentrations in the shaker as a function of time.

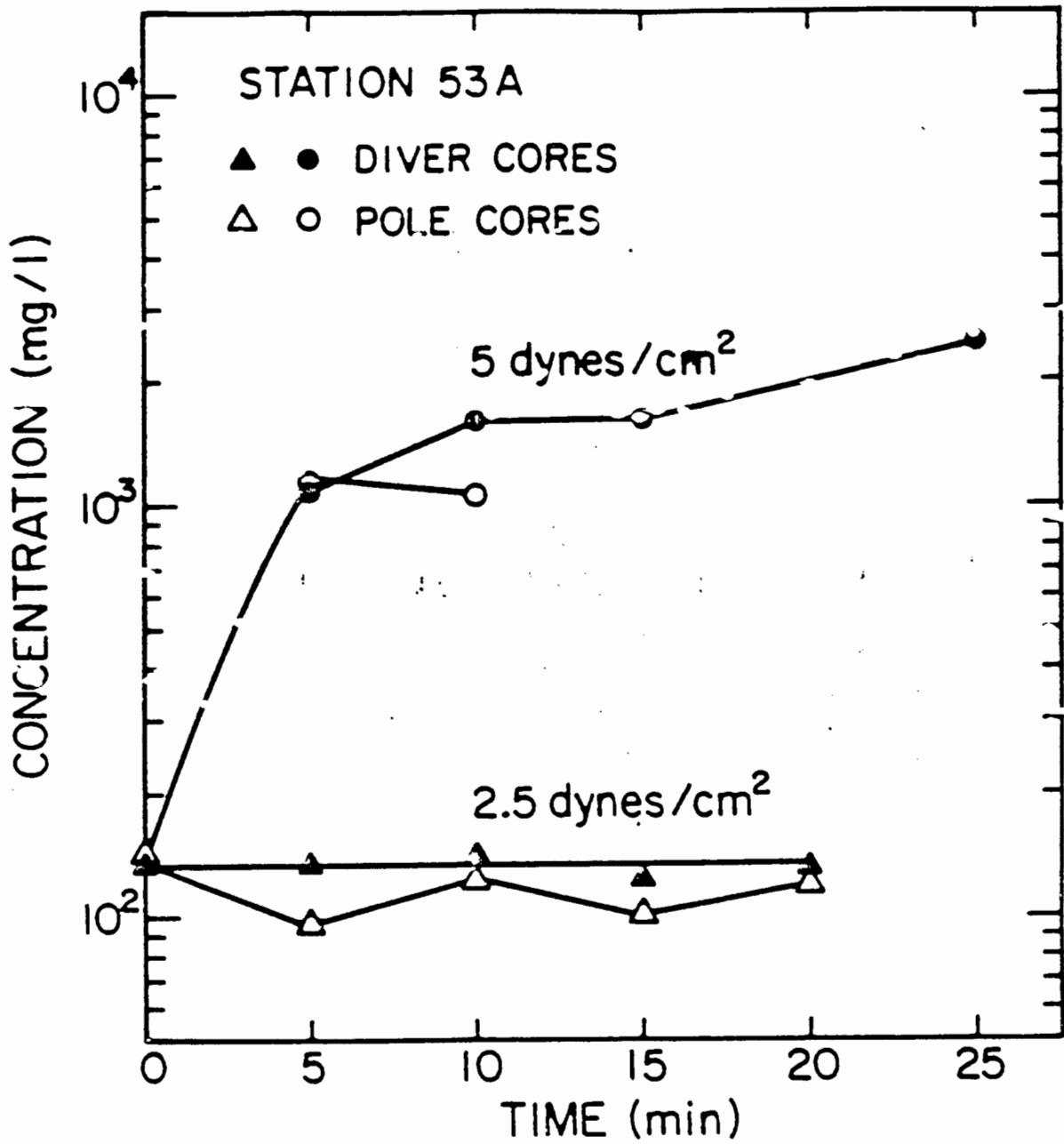


Fig. 12a Comparison tests for the cores obtained by a pole and the cores by a diver.

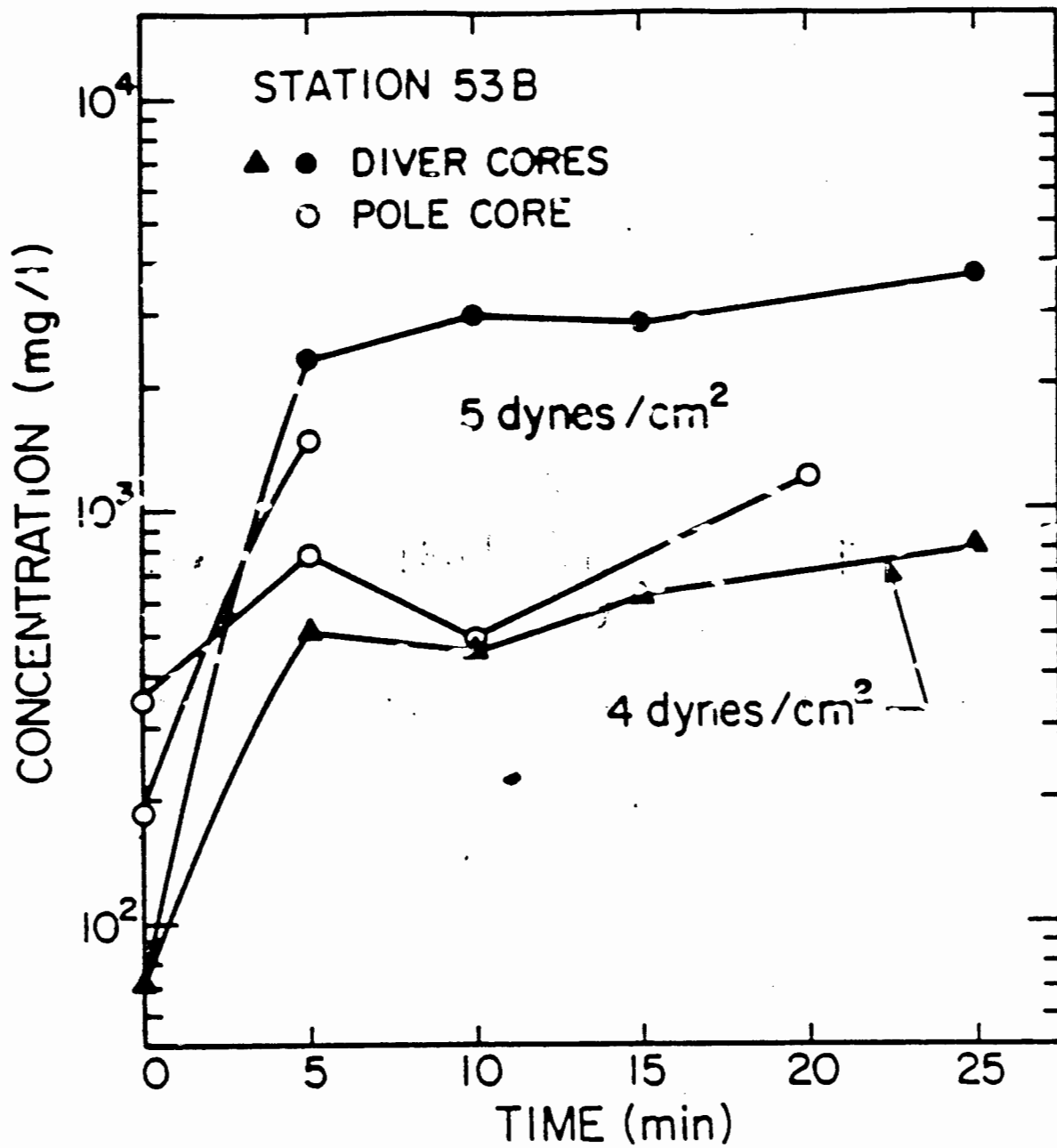


Fig. 12b Comparison tests for the cores obtained by a pole and the cores by a diver.

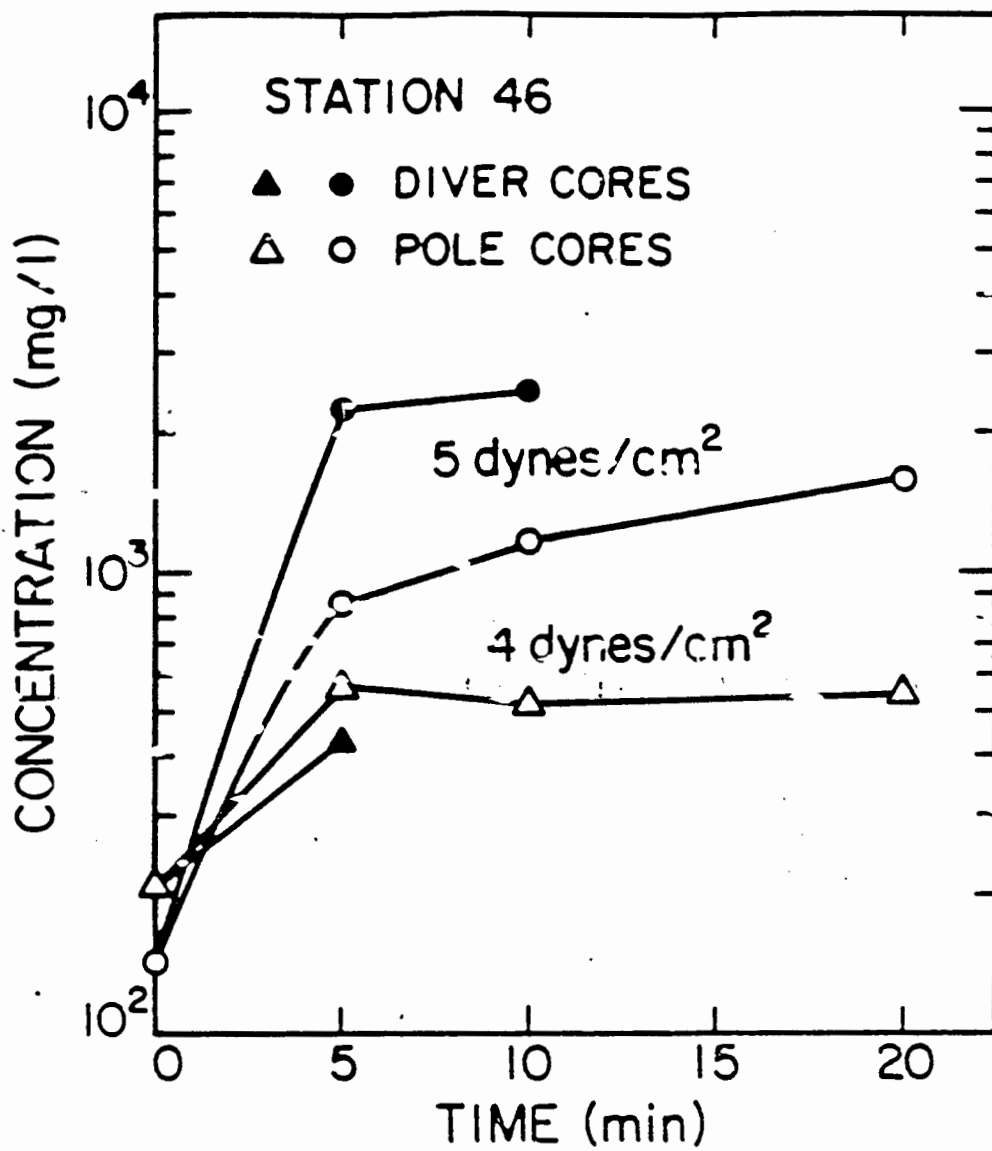


Fig. 12c Comparison tests for the cores obtained by a pole and the cores by a diver.

Table 1. Qualitative description of the sediment samples

STATION #	SEDIMENT DESCRIPTION
30	Brownish silt and clay, sand, oily, petroleum odor
34	Dark coal-like materials, grey collids, oily, petroleum odor
53,53A,53B	sand, algal mat, coal-like particle, weed bit
83	Grey compacted clay and silts, weed
42	Silt layer on top of clay layer, oily, petroleum odor
46	Sand, organic material, algal mat

Table 2 Steady-state concentration for the sediments from each station

STATION #	SHEAR STRESS (dynes/cm ²)	STEADY-STATE CONCENTRATION (Mg/l)
30	2.5	605
30	5	5200
34	2.5	1100
34	5	7500
53	2.5	800
53	5	7000
83	2.5	600
83	5	2600
42	2.5	330
42	5	3250
53A	2.5	140
53A	5	2500(*)
53B	4	800(*)
53B	5	3700(*)
46	4	560
46	5	1600(*)

(*) Steady-state was not reached

THE FLOCCULATION OF FINE-GRAINED LAKE SEDIMENTS
DUE TO A UNIFORM SHEAR STRESS

The flocculation of fine-grained sedimentary particles significantly affects the effective sizes, surface areas, densities, settling velocities, and deposition rates of these particles. Because of this, knowledge of flocculation processes is especially important in such areas as sediment transport, contaminant transport, and waste water treatment. It should be noted that flocculation is a dynamic process with the state of flocculation changing with time and depending on the rates of aggregation and disaggregation of the particles. In turn, these rates depend on state variables such as fluid shear, sediment concentration, dissolved chemicals and salinity, pH, temperature, organic matter, and organisms. However, despite their importance, the processes of aggregation and disaggregation of fine-grained sediments and their dependence on the above parameters are not well understood. To increase the understanding of flocculation is the justification for the present study.

Aggregation of particles occurs as particles within a fluid collide with one another. These collisions are caused predominantly by three processes: Brownian motion, fluid shear, and differential settling. Brownian motion is due to the thermal energy of the fluid and is random in nature. Fluid shear will lead to collisions due to the relative motion between particles caused by this shear. Particles settling at different velocities will also cause collisions as large, faster-settling particles may collide with small, slower-settling particles. These collision processes are relatively well understood.

As particles collide, only a fraction of the collisions will result in cohesion of the particles and the formation or increase in the size of flocs. This probability of cohesion during collisions is determined in part by the forces between particles. However, except through experiments, a quantitative determination of this probability is not possible at present.

The disaggregation of particles also occurs and is due to fluid shear and possibly collisions between particles with sufficient relative translational energy. The rates of disaggregation of fine-grained particles are not well known and must be determined through experiment.

Most of the previous work concerning flocculation has been in the area of waste treatment. In this regard, the strength and density of aluminum-clay flocs where flocculation had been induced by the addition of an aluminum ion solution has been studied (Tambo and Watanabe, 1979; Tambo and Hozumi, 1979). Similar work has been conducted by Boadway (1978), Argamann and Kaufman (1970), and Parker et al. (1972). Delichatsios and Probstein (1975) studied the flocculation of colloidal particles in turbulent pipe flows. Their work was motivated by the importance of learning the behavior, handling, and treatment of dispersions.

In the present study, experiments concerned with the flocculation of fine-grained lake sediments in fresh water were performed. In most regions of a lake, fluid shear is weak and therefore the collision and aggregation of particles is primarily due to Brownian motion and differential settling. However, in certain areas of an aquatic system, such as at and near the air/water interface, the thermocline, the sediment/water interface, and shallow, near-shore areas where wave action is significant, fluid shear is large and will have significant effects on the aggregation and especially disaggregation of particles. These effects are relatively poorly understood.

Because of this, the emphasis of the present study was on the effects of fluid shear on the aggregation and disaggregation of sedimentary particles. In these processes, the effects of sediment concentration are significant and were also investigated.

Factors affecting flocculation are briefly reviewed in the following section. The experiments on flocculation were performed using a Couette type viscometer. This apparatus as well as the experimental procedure is described in subsequent sections and is followed by a discussion of the experimental results.

Factors Affecting Flocculation

In general, the instantaneous size distribution of particles suspended in water is due to both aggregation and disaggregation of these particles and is a time-dependent quantity. In some cases, a steady-state particle size distribution may exist due to a dynamic equilibrium between aggregation and disaggregation but this is an exception.

A general formula for the time rate of change of the particle size distribution can be written as follows. Denote the number of particles per unit volume by n . Approximate the continuous range of particle sizes by discrete size ranges so that the number of particles per unit volume in size range k is n_k . By considering both the aggregation and disaggregation of particles into each size range, one can derive a general formula for the time rate of change of n_k . The result is

$$\frac{dn_k}{dt} = \frac{1}{2} \sum_{i+j=k} \alpha_{ij} N_{ij} - \sum_{i=1}^{\infty} \alpha_{ik} N_{ik} + \sum_{j>k} \gamma_{kj} n_j - \sum_{k>j} \gamma_{jk} n_k \quad (9)$$

where α_{ij} is the probability of cohesion after collision, γ_{ij} is the frequency of disaggregation of flocs with size j into flocs with size i , and N_{ij} is the collision frequency (the number of collisions occurring per unit volume per unit time). This latter quantity can be written as

$$N_{ij} = \beta_{ij} n_i n_j \quad (10)$$

where β_{ij} is the collision frequency function for collisions between particles i and j .

The first term on the right-hand side of Eq. (1) is the rate of formation of flocs by collisions of particles of size i and j . The second term represents the loss of flocs of size k due to collisions with all other particles. The third term represents the rate of increase of n_k due to the disaggregation of flocs of size j and the last term represents the rate of disappearance of flocs of size k due to disaggregation.

The quantities β_{ij} appearing in Eq. (2) are reasonably well known. This function depends on the collision mechanisms of Brownian motion, fluid shear, and differential settling. The original collision rate theories are due to Smoluchowski (1917) while additional work has been done by Camp and Stein (1943). Ives (1978) presents the expressions for the different collision functions as follows.

For Brownian motion,

$$\beta_{ij} = \frac{2}{3} \frac{kT}{\mu} \frac{(d_i + d_j)^2}{d_i d_j} \quad (11)$$

where k is the Boltzmann constant (1.38×10^{-23} Nm/°K), T is the absolute

temperature, μ is the dynamic viscosity of the fluid, and d_i and d_j are the diameters of the colliding particles. For fluid shear,

$$\beta_{ij} = \frac{G}{6} (d_i + d_j)^3 \quad (12)$$

where G is the mean velocity gradient in the fluid. For a turbulent fluid, G can be approximated by $(\epsilon/\nu)^{1/2}$ where ϵ is the energy dissipation and ν is the kinematic viscosity (Saffman and Turner, 1956). For differential settling,

$$\beta_{ij} = \frac{\pi g}{72\mu} (\rho_p - \rho_f)(d_i + d_j)^2 (d_i^2 - d_j^2) \quad (13)$$

where ρ_p is the density of the particles, ρ_f is the density of the fluid, and g is the acceleration due to gravity.

A comparison of collision functions for collisions of an arbitrary particle with a particle of 1 μm diameter is shown in Fig. 13a. For this comparison, the data used was: $T = 20^\circ\text{C} = 293^\circ\text{K}$, $G = 200 \text{ sec}^{-1}$ (2 dynes/cm²), $\rho_p = 2.65 \text{ gm/cm}^3$, and $\rho_f = 1.0 \text{ gm/cm}^3$. As can be seen, Brownian motion is only important for collisions with particles less than 0.1 μm . For particles between 0.1 and 50 μm , collisions are primarily caused by fluid shear, while collisions of 1 μm particles with particles greater than 50 μm are caused chiefly by differential settling. Figure 13b shows the collision function for collisions of an arbitrary size particle with a particle of 25 μm . Again, fluid shear is the dominant mechanism for collisions of particles up to 50 μm .

From the above equations, the β_{ij} 's can be calculated and used to determine the frequency of particle collisions. However to determine dn_k/dt , α and γ must also be known. These quantities are much less well understood. Fluid shear is a major factor in determining γ but its effect has not been

quantified. A major factor in determining the behavior of both α and γ seems to be dissolved chemicals and salinity (Committee on Tidal Hydraulics, 1960; Partheniades, 1980). In natural fresh water, the ions with the most effect are: Na^+ , K^+ , Ca^{+2} , Mg^{+2} , Al^{+3} , Fe^{+2} , Cl^- , SO_4^{-2} , HCO_3^- , and CO_3^{-2} (Faust and Aly, 1981). The cations seem to be most important with the high valence cations more effective as a flocculant than mono-valent cations. The concentrations of Na^+ , Ca^{+2} and Al^{+3} required to flocculate negatively charged particles are approximately in the ratio of $1:10^{-2}:10^{-3}$ (Weber, 1972). Calcium and magnesium seem to be the major cations that influence flocculation in fresh waters.

Other factors that influence flocculation are pH (probably negligible in the usual pH range of 5 to 8 in natural waters (Lambe, 1958)); temperature (less than a factor of 2 effect on settling velocities in the normal temperature range (Lambe, 1958)); and organic matter and organisms (effects may be significant but can not be quantified at the present time). For both α and γ , the size and density of the floc, and therefore the history of formation of the floc, should be significant but the magnitude of this effect is unknown.

Experimental Apparatus

The flocculation experiments were carried out using a Couette type viscometer (van Duuren, 1968; Ives and Bhole, 1977; Boadway, 1978; and Hunt, 1982). This type of viscometer basically consists of two concentric cylinders with one rotating relative to the other. In this way, a velocity gradient is generated in the fluid in the annular gap between the cylinders. The ability to generate a uniform velocity shear is the main advantage of using a Couette viscometer as a flocculator.

The hydrodynamic properties of the Couette device have been discussed by several authors, including Taylor (1923, 1936), Rayleigh (1917), Chandrasekhar (1954), Donnelly (1958), Donnelly and Fultz (1960), and van Duuren (1968). Taylor carried out experimental studies on the stability of the flow inside the annulus. He found that the flow inside the annular gap is more stable with only the outer cylinder rotating and also determined the limiting outer cylinder rotation speed for the flow to remain laminar. Van Duuren gave a detailed account of the derivation of the velocity gradient in the annulus. For only the outer cylinder rotating, the velocity gradient G is

$$G = \frac{2\omega_2 R_1 R_2}{R_2^2 - R_1^2} \frac{1}{r^2} \quad (14)$$

where ω_2 is the angular velocity of the outer cylinder, r the radius in the annulus, and R_1 and R_2 are the radii of the inner and outer cylinders, respectively. By integrating G over the annular width $R_2 - R_1$, one can show that the mean velocity gradient is

$$G_m = \frac{1}{R_2 - R_1} \int_{R_1}^{R_2} G \, dr = \frac{2\omega_2 R_1 R_2}{R_2^2 - R_1^2} \quad (15)$$

By fitting Taylor's experimental data, van Duuren showed that the limiting rotational speed for the outer cylinder was given by

$$\omega_2 = \frac{3.16 \times 10^5 \nu (R_2 - R_1)^{0.7}}{R_2^{2.7}} \quad (16)$$

where ν is the kinematic viscosity. If the rotational speed of the outer cylinder exceeds this limiting value, the laminar flow inside the annulus breaks down and becomes turbulent.

The viscometer used in the present study is shown in Figure 14. The inner radius of the outer cylinder is 2.5 cm and the outer radius of the inner cylinder is 2.3 cm. With these dimensions, the mean shear stress (in dynes/cm²) across the gap becomes $\mu G_m = 0.735/T_2$ where T_2 is the period in seconds of the outer cylinder, and μ is taken to be 1×10^{-2} dynes-sec/cm², the dynamic viscosity of water at 20°C. The theoretical limiting rotation speed of the outer cylinder is then 87 rad/sec or $T_2 = 0.07$ sec. This corresponds to a theoretical maximum mean shear stress of 10.5 dynes/cm². Red food coloring dye was injected into the viscometer to study the flow characteristics. It was found that the dye was rapidly dispersed by turbulent flow when the mean shear stress was larger than 9.2 dynes/cm². For stresses less than this value, the flow inside the viscometer was laminar.

The length of the viscometer was 25.4 cm with a length to gap ratio of 125. The total volume of the annulus was 83 ml. Ideally, the viscometer should be infinitely long to avoid end effects. One way to reduce the end effects is to mount the device vertically with one end open (van Duuren, 1968). However, mounted in this way, the effects of floc sedimentation can become significant. Hence, the viscometer was designed to be mounted horizontally. However, by mounting the viscometer horizontally, the effects of floc settling were not totally removed. The reason for this is that, in addition to the gravitational acceleration, the centrifugal acceleration produced by the rotation of the outer cylinder acts upon the sediment flocs.

An effective maximum acceleration can be obtained by vectorally summing the maximum centrifugal acceleration and the gravitational acceleration.

Then by averaging the magnitude of this combined acceleration over one revolution, an effective acceleration can be obtained (Iacobellis, 1984). By this method, the effective accelerations for the shear stresses used in this experiment (1, 2, and 4 dynes/cm²) were found to be 1.01, 1.14, and 3.19 g, respectively. The effective accelerations for the two smaller shear stresses are not much larger than 1 g. Hence, floc settling is not significant for these stresses.

However, the effective acceleration of 3.19g produced by the 4 dynes/cm² shear stress can not be ignored. This effect is significant if a particle has a density of 2.65 gm/cm³. However, in reality, the effective density of a flocculated particle decreases as the floc size increases due to voids in the flocculated structure (Tambo and Watanabe, 1979; Iacobellis, 1984). For large flocs, this effective density approaches that of water. As can be seen from Eq. (13), the differential settling collision function decreases as the floc density decreases and, in particular, becomes negligible as ρ_p approaches ρ_f . In addition, it was observed in the present experiments that the strengths of the flocs formed by Brownian motion and differential settling were much weaker than those formed in a shear field (also, see Krone, 1984). For these reasons, the effects of differential settling in the experiments were minimal even at the highest stress of 4 dynes/cm² and collisions were due mainly to fluid shear.

The cylinders of the viscometer were made of cast acrylic tubing. The inner cylinder was fixed to a steel shaft through which the viscometer was clamped horizontally to two anchored seats. In the inner cylinder, four intake ports were built in and rubber hoses were connected to these ports. The hoses ran through the steel shaft to the outside of the viscometer. These hoses and intake ports allowed us to inject dye for hydraulic studies.

During flocculation tests, these hoses were clamped. The two end pieces are threaded so that they can be completely removed from the cylinders. In one of the endpieces, a stop-cock was built in. The stopcock enables one to completely remove air bubbles when filling the viscometer with the sediment suspension. A gear was mounted on the other endpiece. Through the coupling of this gear and another gear attached to the shaft of a motor, the outer cylinder was rotated. The motor has a maximum power output of 1/4 horsepower and it was connected to a speed controller. The viscometer can be rotated at periods down to 0.07 sec which corresponds to a mean shear of 10.5 dynes/cm^2 .

The sizes of flocs were measured by use of a Malvern Particle Sizer 3600E. The Malvern Particle Sizer utilizes the Fraunhofer diffraction principle to measure the particle size distribution (Weiner, 1984). The essential components of the sizer are: a light source, a sample cell, Fourier transforming lenses, and a detector. The light source is a 2-mw He-Ne laser beam which is monochromatic and collimated. The sample which contains the floc suspension whose size distribution is to be determined is located in the light path. The light diffracted by the particles are focused by the lens onto the detector. The angle of diffracted light depends on the size of the particle: the smaller the particle, the larger the diffraction angle. Hence, by measuring the light intensity on the detector at various angles from the incident light axis, the particle size distribution can be determined. The detector consists of 30 semi-annular concentric photo diodes. The radii of the diodes are set in such a fashion that the resultant distribution is divided into 15 logarithmically increasing size bands. If one includes the percentage under the lowest size band and the percentages in the 15 size bands, one can obtain a 16 size band distribution. The main advantage of using a Malvern Particle Sizer is that flocs are not forced through a

narrow gap at any time and hence are not disaggregated during the measurement.

Experimental Procedure

The material used in this experiment was a fine-grained sediment from the mouth of the Detroit River as it enters Lake Erie. The sediments were analyzed by X-ray diffraction and found to be composed of calcite, chlorite, dolomite, illite, kaolinite, montmorillonite, potassium feldspar, and quartz.

In order to obtain a fine-grain sediment suspension that had uniform properties from one test to the next, the following procedures were followed. About 10 kg of the sediment were stored with water at an average concentration of 100 gm/l. The container was kept covered so that the sediments were in the dark. About 24 hours prior to each experiment, the sediments inside the container were thoroughly mixed by a plunger. Just before each test, the sediments were stirred again and 100 ml of sediment slurry were taken out and placed into a 1 liter graduated cylinder with 900 ml of tap water. The diluted slurry in the cylinder was then thoroughly mixed and allowed to settle for seven minutes. After this time, 30 to 150 ml of the top portion of the mixture was removed and placed into a beaker with 400 ml of water. The concentration of this suspension was then measured and the suspension was diluted again until it had the desired concentration. The last step in the preparation of the initial floc suspension was to break up the flocs by means of a blender.

The size distribution of the initial suspension was then measured and was found to be rather uniform between tests. Typical size distributions for concentrations of 50 and 800 mg/l are shown in Figure 15. In general, the median floc diameter ranged from 3.1 to 4.7 μm , depending on the concentra-

tion, and the maximum floc size was 23.7 μm . It was felt that this type of size profile more closely resembles the size profile likely to be entrained by shear stresses within our experimental range than would the size profile of the original sediments.

As mentioned earlier, dissolved chemical ions may affect the processes of flocculation. In order to ensure that the water used to dilute the sediment suspension was the same for every test, the tap water obtained for the first test was stored in a covered container. The whole series of experiments were completed in two weeks. It was believed that the water quality did not change appreciably in this time period. The experimental results were reproducible and confirmed this belief. The tap water was analyzed by the Montgomery Laboratory in Pasadena, California about one month after the first day of the experiment. The major ion contents of this water are listed in Table 3 (series A). pH of this tap water was not determined but, according to the local water treatment plant, was about 7. During the tests, the water in the viscometer had a temperature ranging from 19 to 23°C.

After the size distribution of the initial floc suspension was taken, the suspension was poured into the viscometer. With the stopcock on the device open, a syringe filled with the suspension was connected to one of the hoses fixed to an intake port and additional suspension was slowly pumped into the annulus until all the air bubbles had escaped. After this, the viscometer was clamped onto the anchored seats and was slowly brought up to the speed corresponding to the desired shear stress.

Under some conditions, it was found that the flocs inside the annulus were gradually pushed to the outer cylinder by the centrifugal force. In order to avoid this, the viscometer was slowly brought to a stop about every five minutes. At this time, about 9 ml of the suspension was withdrawn from the viscometer by use of a syringe. The viscometer was then slowly and

gently rocked from one end to the other while it was also being rotated around its long axis. After this mixing, the viscometer was either refilled for running or opened up for sampling.

The sampling of the floc suspension in the viscometer was carried out every 5 to 20 minutes of running time, depending on how fast the size distribution changed. For sampling, the viscometer was brought to a vertical position. The top endpiece was unscrewed and the inner cylinder was carefully pushed to one side. Connected to a pipette, a nylon tubing with an outer diameter of 3.73 mm and an inner diameter of 2.92 mm was inserted into the annulus for sample retrieval. Depending on the concentration of the suspension, 0.6 to 8 ml of suspension was removed from the viscometer. For accurate measurements, the samples were taken from four positions equidistant from each other. These were then placed into the sample cell of the Malvern Particle Sizer and diluted with de-ionized water. Ideally, the samples should be diluted with filtered working water. However, tests had been conducted to compare the size distribution measured with a floc suspension diluted with de-ionized and filtered tap water. No difference in size distribution was detected. As the size distribution was being measured, the viscometer was refilled with the suspension which had been withdrawn previously. The viscometer was also replenished with the initial suspension to account for the volume loss during the measurement. The viscometer was then restarted.

The time period between the stopping and restarting of the viscometer was about 4 to 5 minutes. During this time, the viscometer was idle and the flocs in the annulus flocculated very slightly due to settling. As mentioned earlier, the flocs formed by settling were easily broken up by the applied shear when the viscometer was restarted. The result was that the flocs formed during the idle time of the viscometer did not create a problem.

Results

The usual experiment was a double shear stress test and was conducted as follows. The sediments in the viscometer were initially disaggregated. The viscometer was then operated at a constant shear stress for about two hours. During this time, the sediments in the viscometer flocculated with the median particle size initially increasing rapidly with time but then more slowly until a steady-state was reached where the median particle size remained approximately constant with time. This always occurred in times less than two hours. After this steady-state, the shear stress of the viscometer was changed to a new value and kept there for another two hours. Again, after an initial transient of less than two hours, a new steady-state was reached. The initial shear stresses were 1, 2, and 4 dynes/cm² and these were changed to 2, 4, and 1 dynes/cm² respectively. The experiments were run at sediment concentrations of 50, 100, 400, and 800 mg/l.

For this type of test and for a concentration of 100 mg/l, the median particle diameters as a function of time are shown in Figure 16. The initial diameters were about 3.5 μm . It can be seen that, for each shear, the particle size initially increased relatively slowly. After about 15 minutes, the size increased more rapidly but then approached a steady-state in about an hour. For the 1, 2, and 4 dynes/cm² tests, the steady-state median diameters were about 115, 80, and 50 μm while the steady-state was reached in about 100, 80, and 60 minutes. There were fluctuations about this steady-state with the larger fluctuations occurring at the lower stresses.

After the change in shear stress, a transient occurred after which a new steady-state was reached. For a particular shear stress, it can be seen that the median particle size for the second steady-state is approximately the

same as the median particle size after the first steady-state. This indicates that the steady-state median particle size for a particular shear is independent of the manner in which the steady-state is approached.

From Figure 16, it can be seen that the floc size increases as the shear decreases. From visual and microscope observations, it can be shown that the flocs formed at the lower shears are fluffier, more fragile, and have lower effective densities than do the flocs formed at the higher shears.

The steady-state size distributions for the above tests are shown in Figure 17. The distributions shown are the averages of the size distributions during the first steady-state. Size distributions during the second steady-state were similar. The differences in size distributions for different shear stresses are clearly seen with the sediments at the lowest stress having the largest percentage of large flocs and the smallest percentage of small particles and vice versa for the sediments at the highest stress.

Figures 18 and 19 show results for a sediment concentration of 400 mg/l. The behavior shown is qualitatively similar to that shown in Figures 16 and 17 for a sediment concentration of 100 mg/l. Figure 18 shows that the median steady-state particle diameters for 1, 2, and 4 dynes/cm² are now 60, 40, and 20 μ m respectively, values which are approximately half those for 100 mg/l. The results again show that the steady-state floc diameter is independent of the history of the applied stress. The first steady-state is reached in approximately 60, 40, and 40 minutes for the three stresses, somewhat faster than the tests at 100 mg/l. Figure 19 shows the particle size distributions for 400 mg/l and is qualitatively similar to Figure 12.

In order to see the effect of sediment concentration on flocculation, the time histories of the median diameters from tests with a stress of 2 dynes/cm² were determined. These are shown in Figure 20. Included in the

figure are tests with concentrations of 50, 100, 400, and 800 mg/l, where the tests with 50 and 800 mg/l concentrations are ones with a single applied stress. The curves for the 100 and 400 mg/l tests are the ones shown in Figures 16 and 18, respectively, with the 2 dynes/cm^2 stress and before the stress change. The two upper curves are the results of the tests with 50 and 100 mg/l concentration and are qualitatively similar to each other. The median diameters for these tests do not change much in the first 15 minutes and then increase rapidly. After about 50 minutes, the median diameters reach a quasi-steady-state but with large fluctuations present. The two lower curves are for the two larger concentrations of 400 and 800 mg/l and are also qualitatively similar to each other. The steady-state is reached in approximately 30 minutes with relatively little fluctuations thereafter. The steady-state median diameters are 100, 80, 40, and 26 μm for the tests with concentrations of 50, 100, 400, and 800 mg/l, respectively. This clearly indicates that there is a marked influence of the floc concentration on the sizes of the flocs, i.e., the less the floc concentration, the larger the flocs.

Plotted in Figure 21 are the averaged steady-state size distributions for a shear stress of 2 dynes/cm^2 . It can be seen that, for the same applied stress, the sediments have a higher percentage of large flocs and a lower percentage of small particles when the concentration is lower.

The large flocs present in these experiments were quite fragile. A schematic diagram of a typical floc is shown in Figure 22. It can be seen that individual particles (usually on the order of 1 μm in diameter) are relatively closely and therefore strongly bound together into clumps. Several of these clumps are then loosely and therefore relatively weakly bound to each other to form a floc. Because of this fragility, great care must be taken in measuring and handling this material. In the present study,

our procedures were continually modified until it was felt that the procedures had no significant effect on the final experimental results.

Additional experiments were run besides those described above. First, several duplicate experiments were made to test the reproducibility of the experiments. In all cases, the results were reasonably well reproduced: for example, the steady-state median particle diameters for duplicate tests differed by less than 10%.

Another series of experiments was made with the same sediments but with slightly different water (a mixture of well water with added chemical salts). The composition of this water (series B) is compared with the water used in the reference experiments (series A) in Table 3. The series B experiments were identical to the series A experiments. The results for the steady-state median particle diameter for both series are compared in Table 4. Although there are modest differences, the results are generally similar. This tends to indicate that small changes in fresh water composition do not have major effects on flocculation. Of course, these later tests are only suggestive and much additional work is needed before this conjecture can be proved or disproved.

Summary and Concluding Remarks

Flocculation has a significant effect on the effective sizes, surface areas, densities, settling velocities, and deposition rates of fine-grained sediments and hence is important in determining the transport and fate of not only sediments but contaminants as well. It should be emphasized that flocculation is a dynamic process with both aggregation and disaggregation of particles occurring continuously.

The effects of fluid shear on the rate of aggregation and disaggregation of fine-grained sediments are of major importance in lakes but are not well understood. In the present study, experiments were performed to investigate these effects. A Couette viscometer was used to apply a uniform shear stress to the sediment suspension. A series of experiments were made for shear stresses of 1, 2, and 4 dynes/cm² and for sediment concentrations from 50 mg/l to 800 mg/l, values which are characteristic of those found in the Great Lakes.

The particle size distribution as a function of time was determined. Quantitative results were obtained for the decrease in steady-state floc size with increasing shear stress and with increasing sediment concentration. For example, the steady-state median floc diameter changed from 110 μ m to 50 μ m as the shear stress changed from 1 dyne/cm² to 4 dynes/cm² (when the sediment concentration was 100 mg/l) and changed from 100 μ m to 25 μ m as the sediment concentration changed from 50 mg/l to 800 mg/l (when the shear stress was constant at 2 dynes/cm²). The times required for flocculation to occur under different conditions were also determined and were typically on the order of an hour, again dependent on the shear and sediment concentration.

Experiments were performed such that the steady-state was approached in different ways. It was found that the steady-state particle size distribution was independent of its history. Of course, this makes a theoretical analysis involving flocculation much easier.

The present experiments gave information on the effects of fluid shear on particle size. However, in order to predict the transport of particles, it is also necessary to know the settling speeds of these particles. If a particle is spherical with known density, the size and settling speed are related by the well-known Stokes' law, which is

$$w_s = \frac{gd^2}{18\mu} (\rho_p - \rho_f) \quad (9)$$

The formula is valid for settling speeds such that the Reynolds' number ($Re = \rho_f w_s d / \mu$) is less than about 0.5, i.e., for sedimentary particles with a diameter less than about 100 μm . However, for flocculated particles, the effective density of the floc can be quite different from the density of each individual particle. In fact, preliminary evidence (Iacobellis, 1984) indicates that the effective density for large flocs approaches that of water and therefore the settling speed is relatively small. When the effective density is not known, the diameter and settling speed are not related by Stokes' law. In fact, they are not even uniquely related to each other so that each parameter must be determined independently.

Obviously, considerable work needs to be done before flocculation of fine-grained sediments is adequately understood. Parameters that affect flocculation and which need further investigation are sediment mineralogy, water quality, organic matter, and organisms. In addition, the parameters that relate particle size and speed need to be determined.

TABLE 3. DISSOLVED ION COMPOSITION (mg/l)

	<u>Series A</u>	<u>Series B</u>
Na ⁺	44.9	78.2
K ⁺	2.4	7.8
Ca ⁺²	74.1	146
Mg ⁺²	38.0	37.4
Al ⁺³	<0.02	<0.02
HCO ₃ ⁻	171	165
CO ₃ ⁻²	0.07	0.07
Cl ⁻	23	200
SO ₄ ⁻²	250	250

TABLE 4. STEADY-STATE MEDIAN DIAMETERS (μm)

	<u>Series A</u>	<u>Series B</u>
50 mg/l, 2 dyn	100	
100 mg/l, 1 dyn	105	95
100 mg/l, 2 dyn	80	75
100 mg/l, 4 dyn	50	43
400 mg/l, 1 dyn	60	56
400 mg/l, 2 dyn	40	30
400 mg/l, 4 dyn	20	16
800 mg/l, 2 dyn	20	

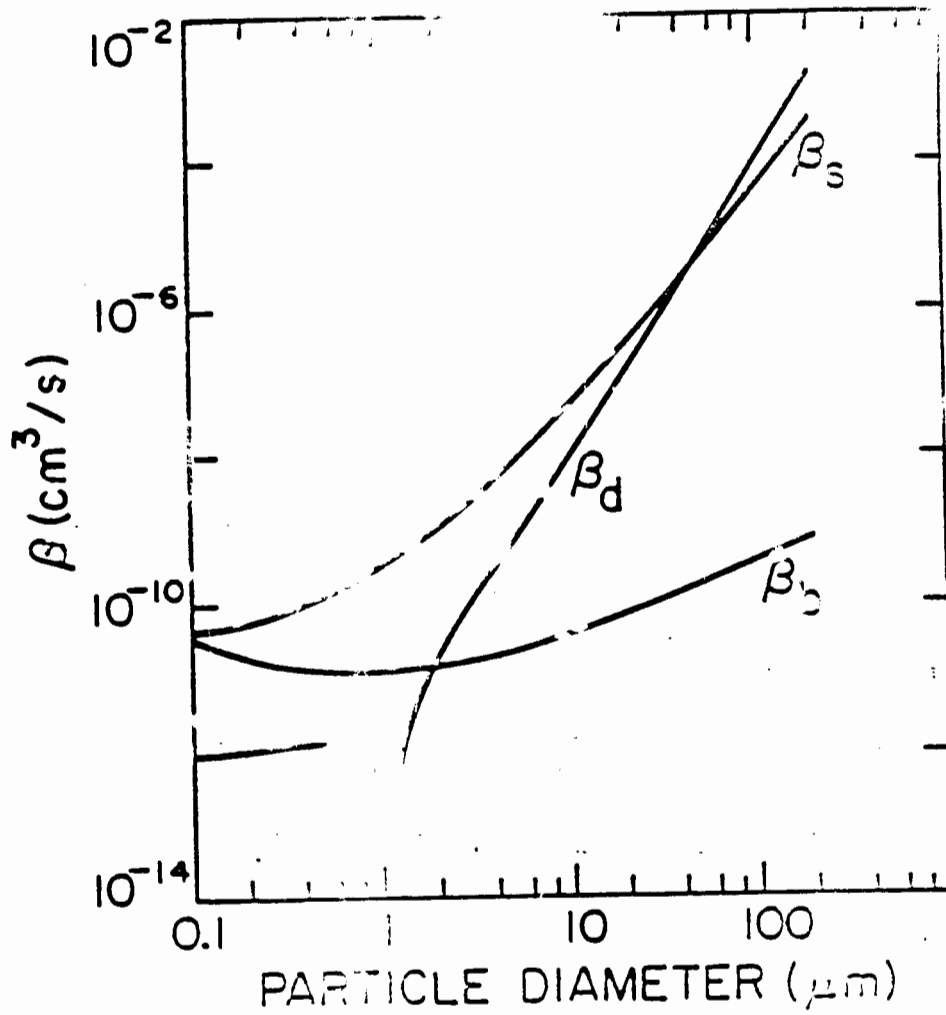


Figure 13. Collision function β as a function of particle size. Collisions with a $1 \mu\text{m}$ particle. β_s is the collision function due to shear, β_d is the collision function due to differential settling, and β_b is the collision function due to Brownian motion. For these calculations, $T = 293^\circ\text{K}$, $G = 2 \text{ dynes/cm}^2$, and $\rho_p - \rho_f = 1.65 \text{ gm/cm}^3$.

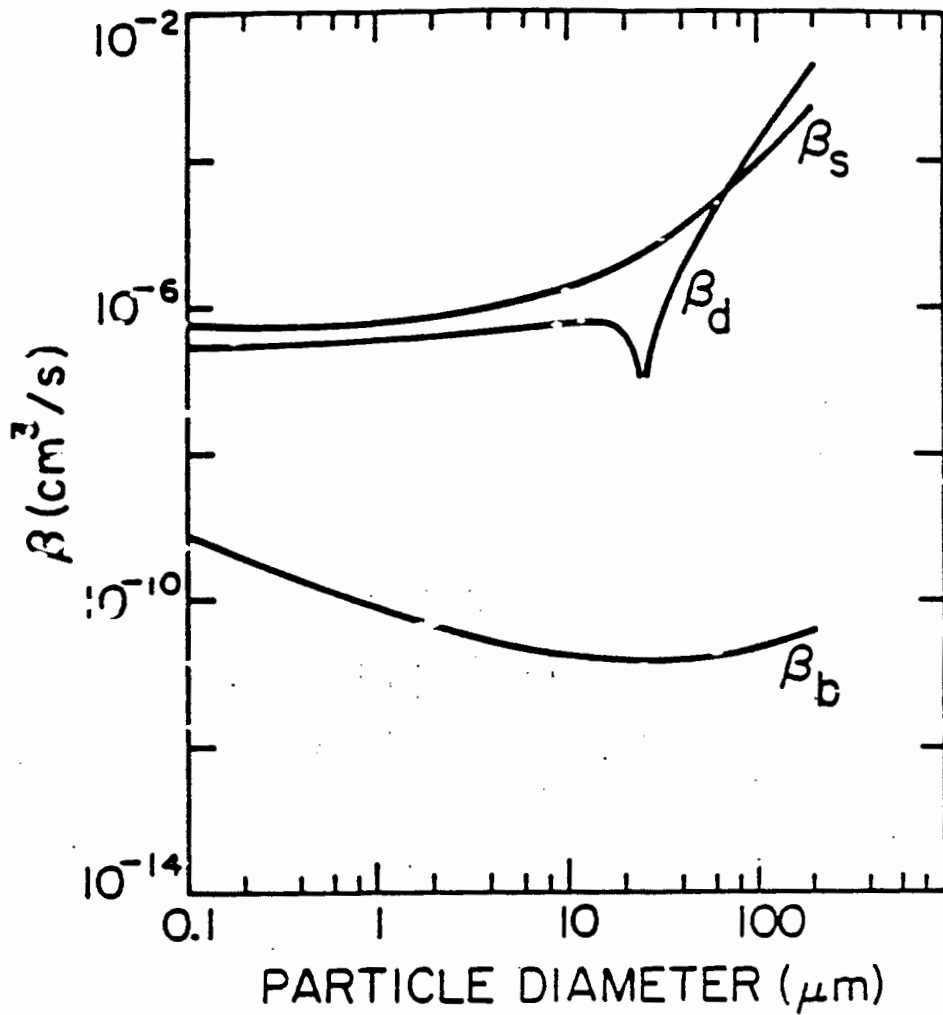


Figure 13. Collision function β as a function of particle size. Collisions with a 25 μm particle. β_s is the collision function due to shear, β_d is the collision function due to differential settling, and β_b is the collision function due to Brownian motion. For these calculations $T = 293^\circ\text{K}$, $G = 2$ dynes/ cm^2 , and $\rho_p - \rho_f = 1.65$ gm/ cm^3 .

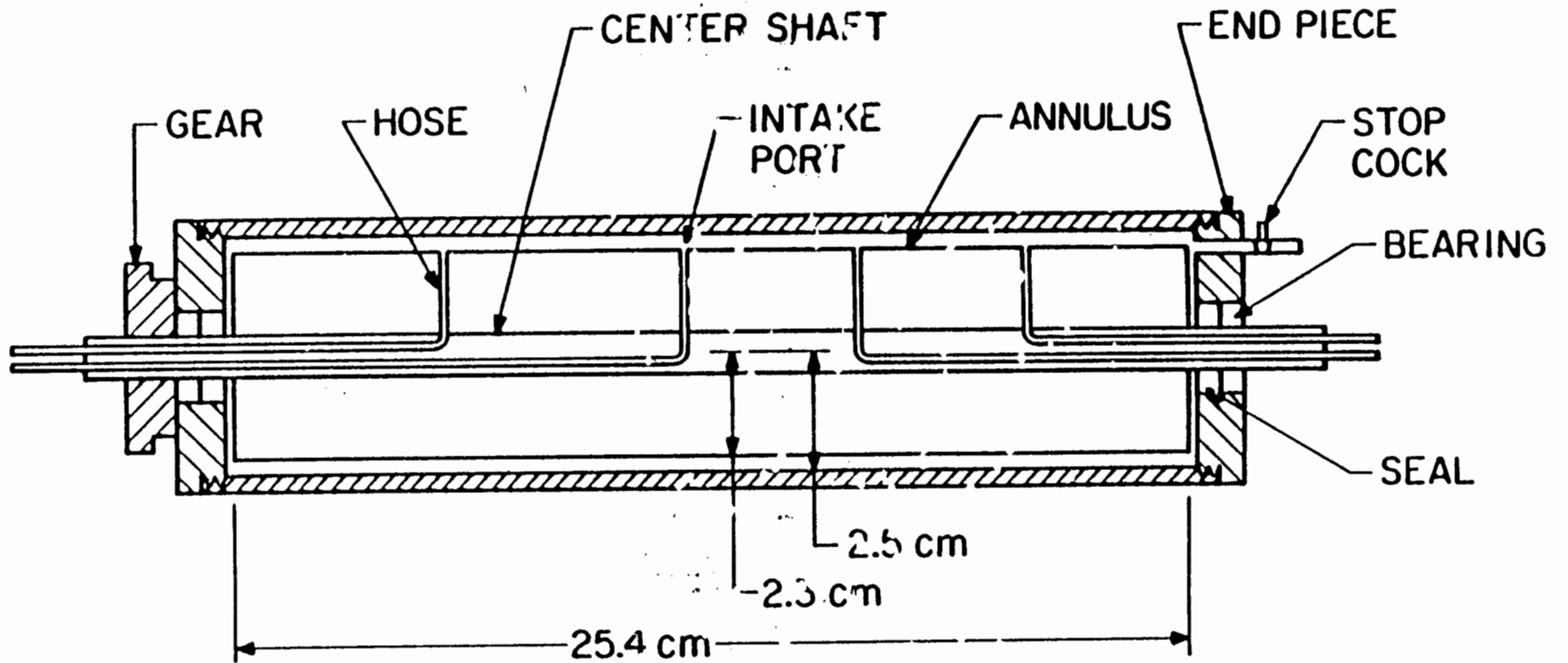


Figure 14. A schematic of the viscometer.

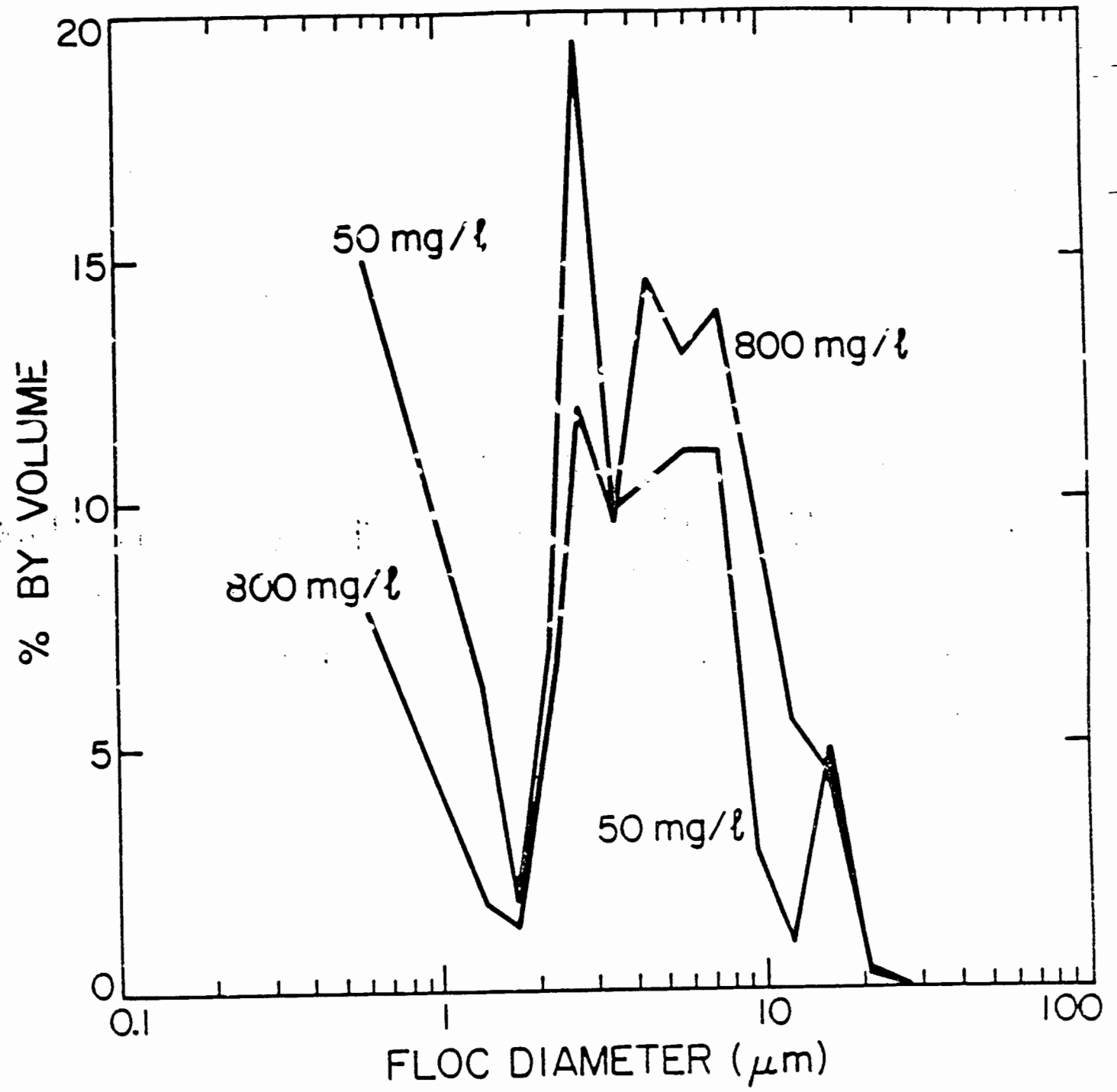


Figure 15. Typical size distributions of the initial suspension.

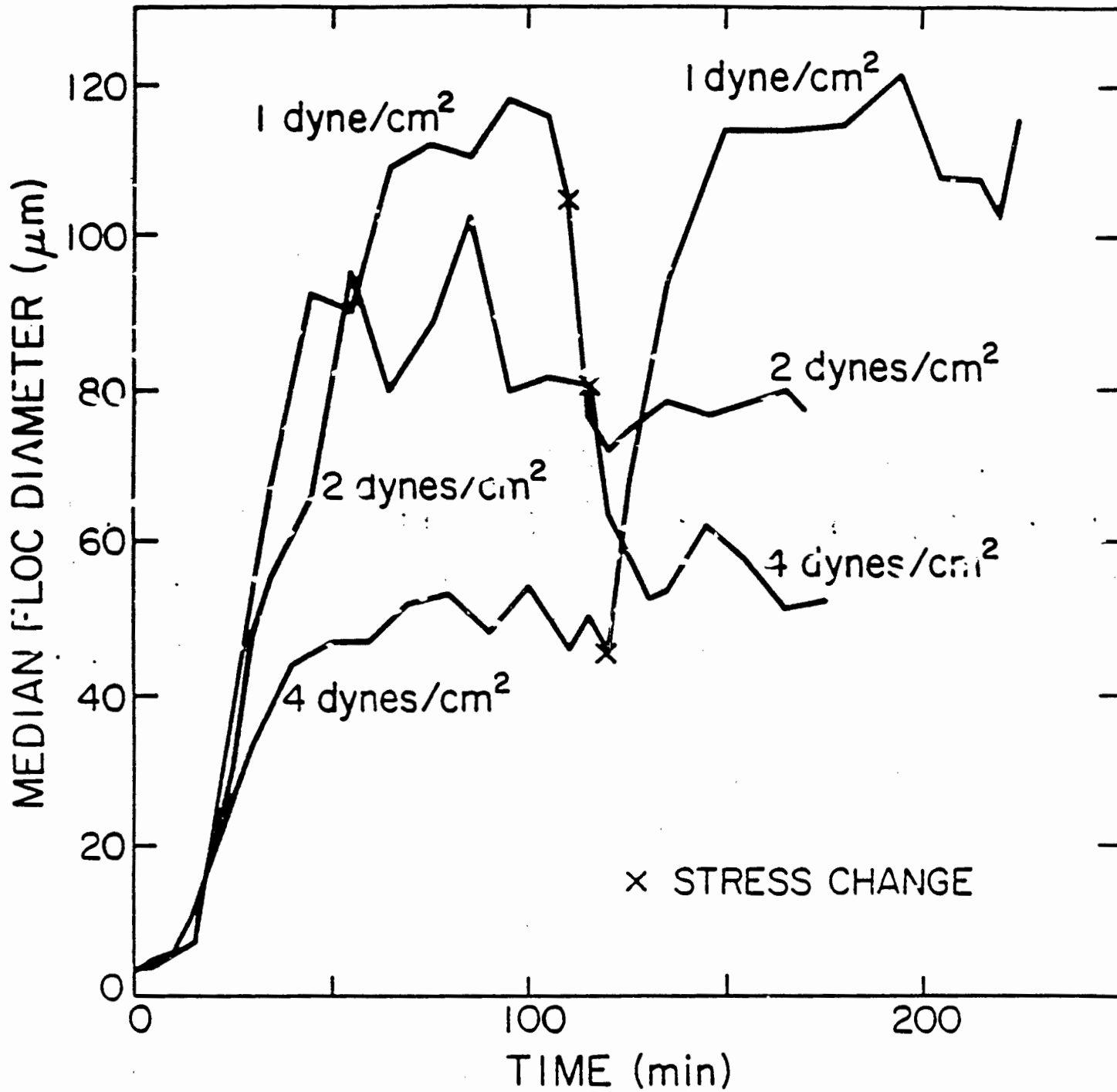


Figure 16. Time variations of median floc diameters for the tests with 100 mg/l floc concentration.

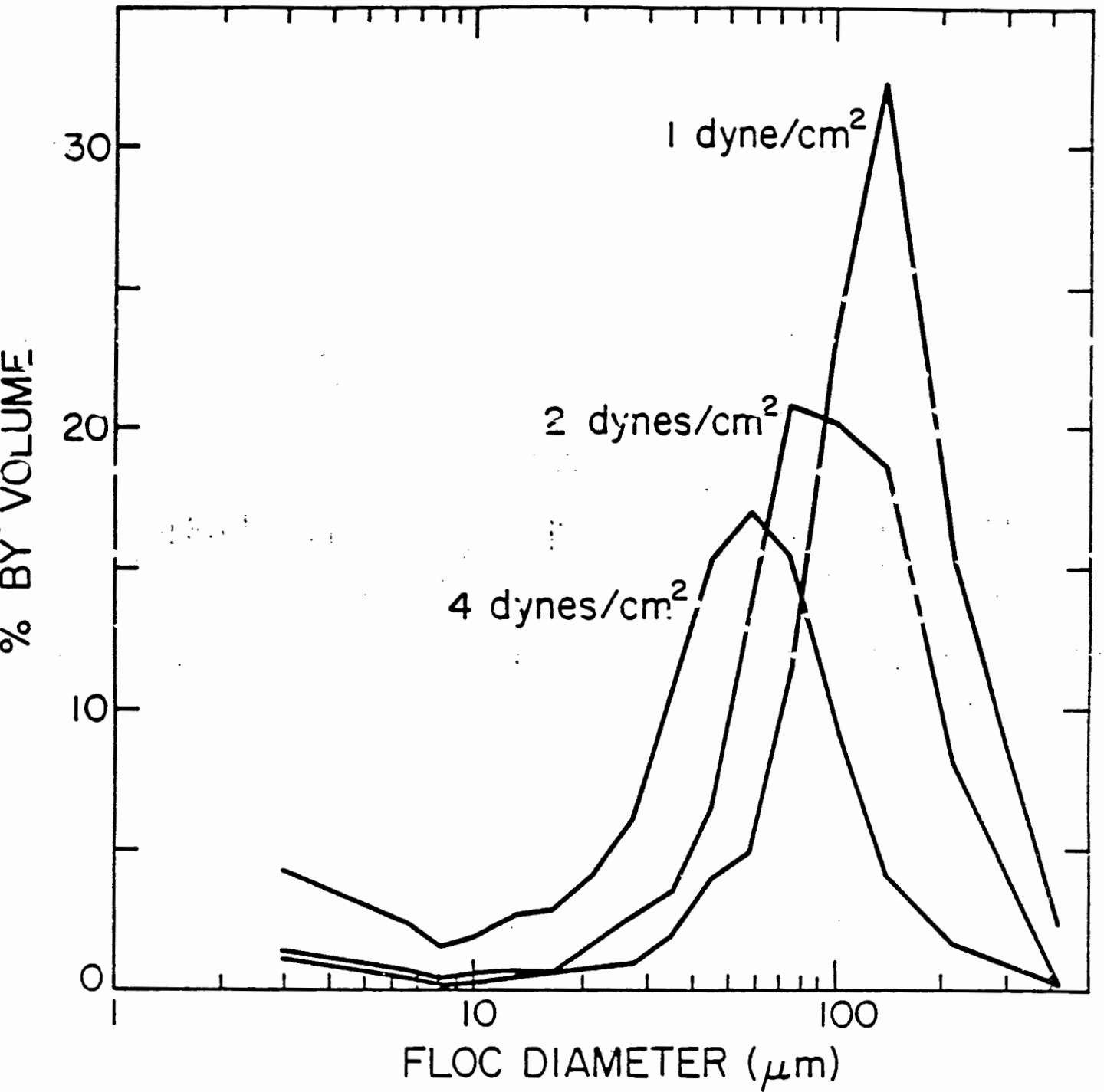


Figure 17. Averaged steady-state floc size distributions for the tests with 100 mg/l floc concentration.

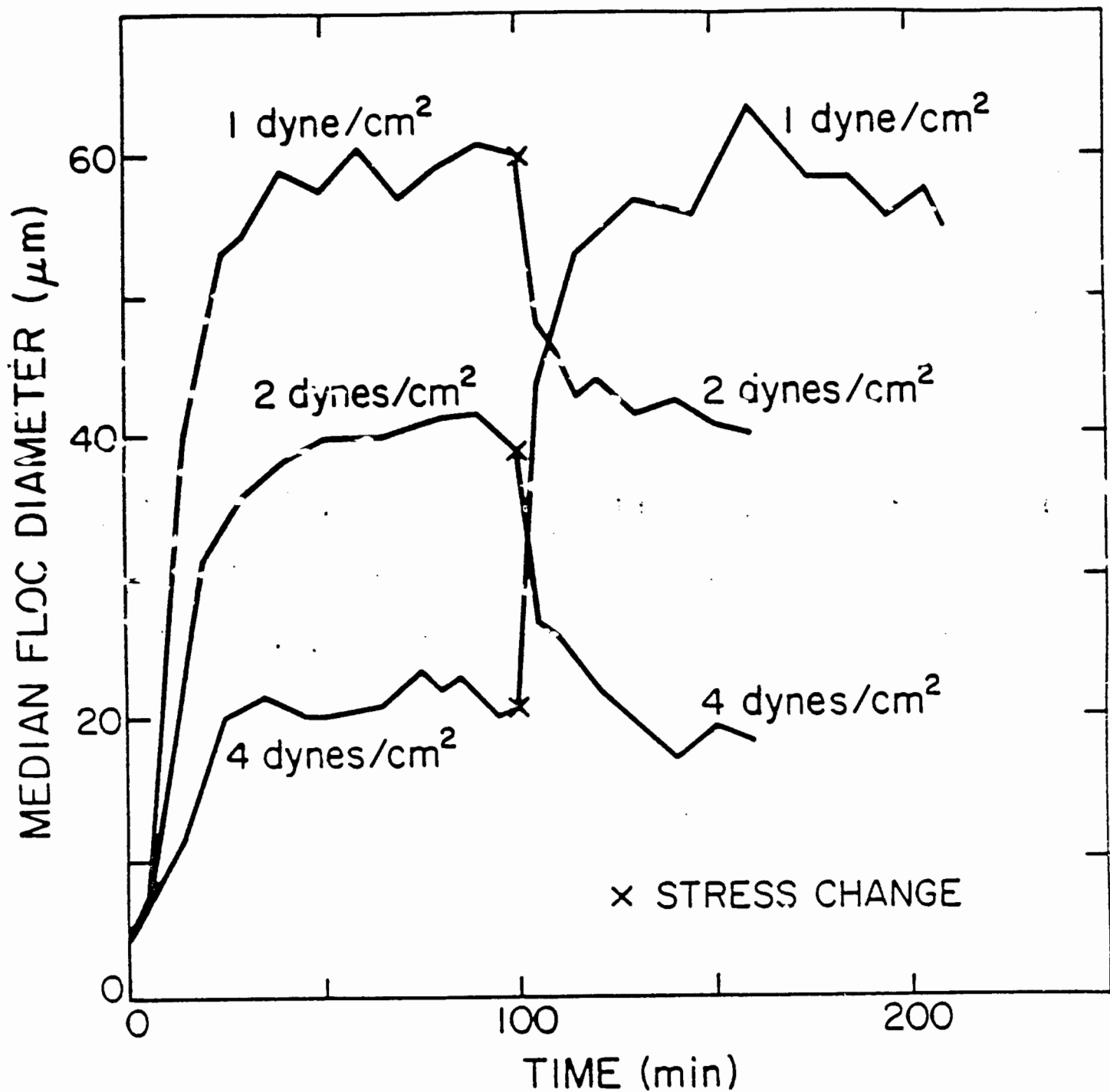


Figure 18. Time variations of median floc diameters for the tests with 400 mg/l floc concentration.

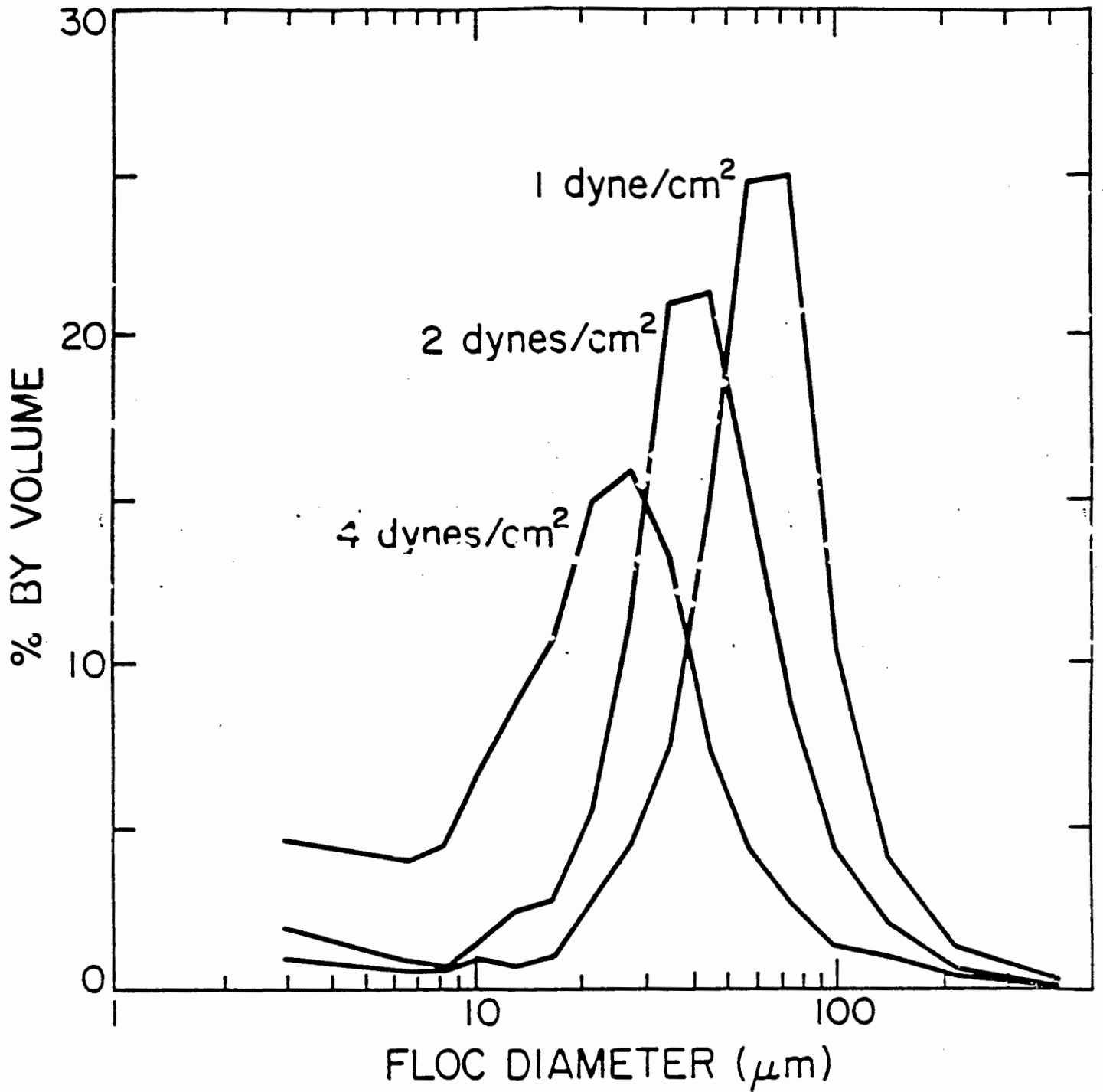


Figure 19. Averaged steady-state floc size distributions for the tests with 400 mg/l floc concentration.

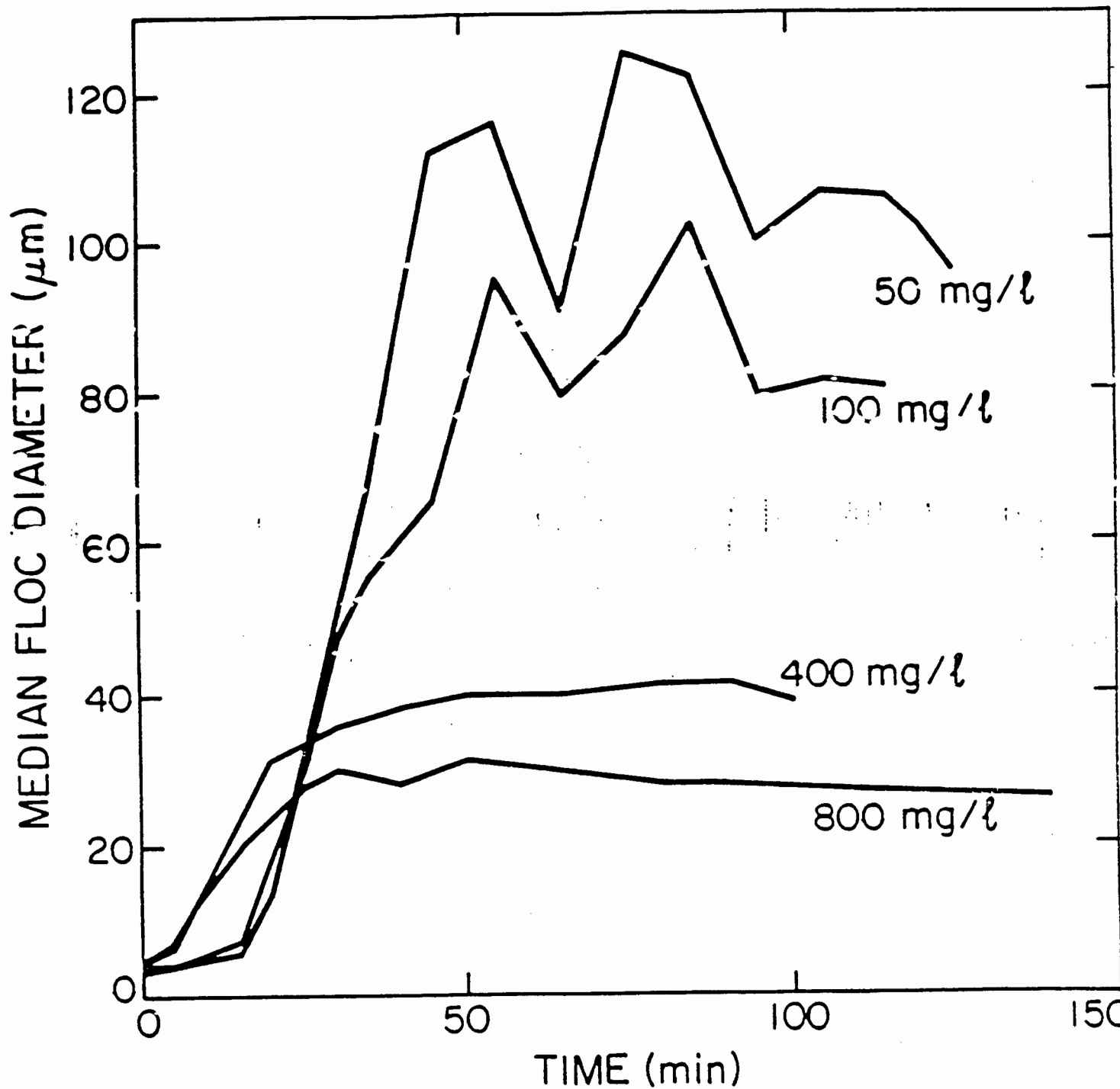


Figure 20. Time variations of median floc diameters for the tests with an applied shear stress of 2 dynes/cm².

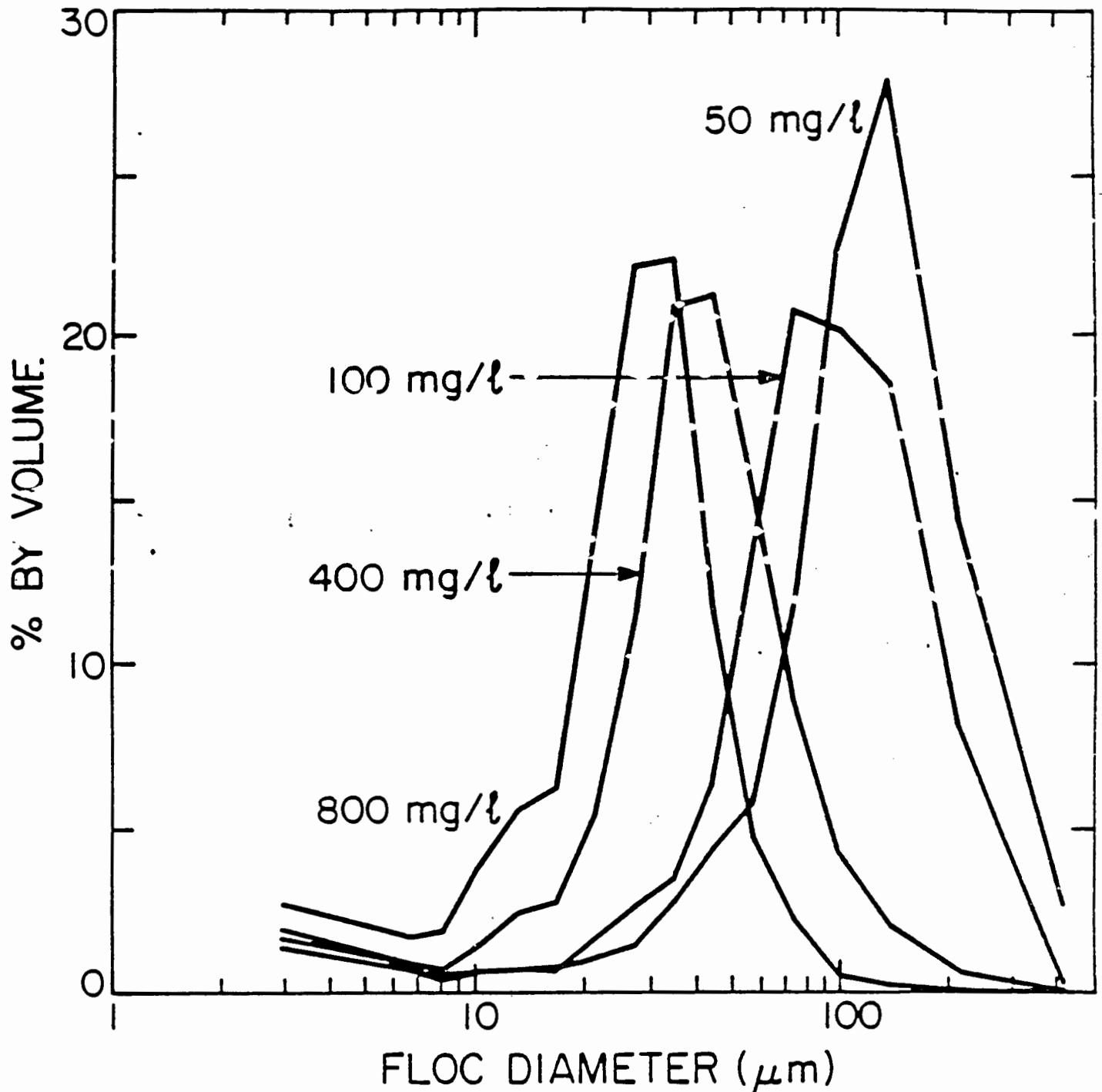


Figure 21. Averaged steady-state floc size distributions for the tests with an applied shear stress of 2 dynes/cm².

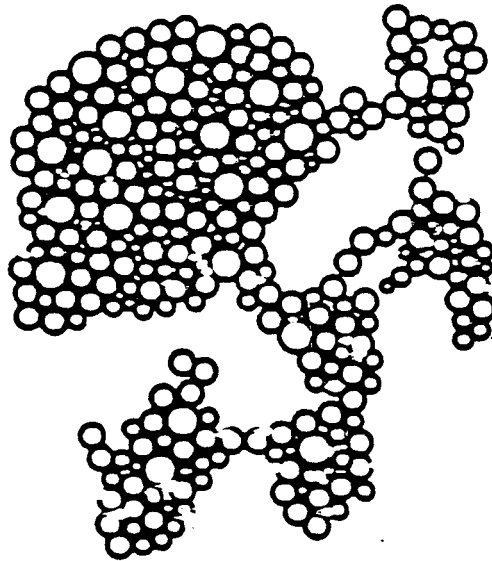


Figure 22. Schematic diagram of a typical floc.

REFERENCES

- Argamann, Y. and Kaufman, W.J., 1970. "Turbulence and Flocculation," Journal of the Sanitary Engineering Division, Vol. 96, pp. 223-241.
- Boadway, J.D., 1978. "Dynamics of Growth and Breakage of Alum Floc in Presence of Fluid Shear," Journal of the Environmental Engineering Division, Vol. 104, pp. 901-915.
- Camp, T.R. and Stein, P.C., 1943. "Velocity Gradients and Internal Work in Fluid Motion," Journal of the Boston Society of Civil Engineers, Vol. 30, No. 4, pp. 219-237.
- Chan, R., 1977. Finite Difference Simulation of the Planar Motion of a Ship, Second International Symposium on Computational Ship Hydrodynamics, pp. 39-52.
- Chandrasekhar, S., 1954. "The Stability of Viscous Flow Between Rotating Cylinders." *Mathematika*, Vol. 1, pp. 5-13.
- Committee on Tidal Hydraulics, 1960. Soil as a Factor in Shoaling Processes: A Literature Review, Technical Bulletin No. 4, U.S. Army Corps of Engineers.
- Delichatsios, M.A. and Probstein, R.F., 1975. "Coagulation in Turbulent Flow: Theory and Experiment," *Journal of Colloid and Interface Science*, Vol. 51, No. 3, pp. 394-405.
- Donnelly, R.J., 1958. "Experiments on the Stability of Viscous Flow Between Rotating Cylinders I: Torque Measurements," *Proceedings, Royal Society, London, Series A*, Vol. 246, pp. 312-325.
- Donnelly, R.J. and Fultz, D., 1960. "Experiments on the Stability of Viscous Flow Between Rotating Cylinders II: Visual Observations," *Proceedings, Royal Society, London, Series A*, Vol. 258, pp. 101-123.
- Engquist, B. and A. Majda, 1977. Absorbing Boundary Conditions for the Numerical Simulation of Waves, *Mathematics of Computation*, 31:629-651.
- Faust, S.D. and Aly, O.M., 1981. "Chemistry of Natural Waters," Ann Arbor Science Publications, Inc.
- Fukuda, M.J. and Lick, W., 1980. "The Entrainment of Cohesive Sediments in Freshwater," *Journal of Geophysical Research*, Vol. 85, No. C5, pp. 2813-2824.
- Hunt, J.R., 1982. "Self Similar Particle-Size Distributions During Coagulation: Theory and Experimental Verification," *Journal of Fluid Mechanics*, Vol. 122, pp. 169-185.

- Iacobellis, S., 1984. "The Flocculation of Fine-Grained Lake Sediments Subjected to a Uniform-Shear Stress," Master's thesis, University of California, Santa Barbara.
- Ives, K.J., 1978. "Rate Theories," The Scientific Basis of Flocculation, ed. K.J. Ives, Sijthoff and Noordhoff International Publishers, B.V., Alphen aan den Rijn, The Netherlands, pp. 37-61.
- Ives, K.J. and Bhole, A.G., 1977. "Study of Flowthrough Couette Flocculators--II. Laboratory Studies of Flocculation Kinetics," Water Research, Vol. 11, pp. 209-215.
- Kreiss, H.O., 1966. Proceedings of a Symposium at the University of Wisconsin, D. Greenspan, ed., Wiley, New York.
- Yrone, R.B., 1974. The Significance of Aggregate Properties to Transport Processes, in Estuarine Cohesive Sediment Dynamics, ed. A.J. Mehta, Springer-Verlag Inc., pp. 66-84.
- Lambe, T.W., 1958. "The Structure of Compacted Clay," Journal of Soil Mechanics and Foundation Division, ASCE, Vol. 84, No. SM2.
- Lee, D.Y., Lick, W. and Kang, S.W., 1981. "The Entrainment and Deposition of Fine-Grained Sediments in Lake Erie," Journal of Great Lake Research, Vol. 7, No. 3, pp. 224-233.
- Lick, W., 1982. Entrainment, Deposition and Transport of Fine-Grained Sediments in Lakes, Hydrobiologia, 91:31-40.
- Lick, W. and S.W. Kang, 1987. Entrainment of Sediments and Dredged Materials in Shallow Lake Waters," J. Great Lakes Research, in press.
- Lick, W., K. Ziegler and J. Lick, 1986. Interior and Boundary Difference Equations for Hyperbolic Differential Equations, Numerical Methods for Partial Differential Equations, 2, pp. 157-172.
- Lick, W., K. Ziegler and J. Lick, 1987. Open Boundary Conditions for Hyperbolic Equations, Numerical Methods for Partial Differential Equations, 3, pp. 101-115.
- MacIntyre, S., Lick, W., and Tsai, C.H., 1986. "Entrainment of Cohesive Riverine Sediments," EPA Report, Large Lakes Research Station, Grosse Ile, Michigan.
- Mehta, A.J. and Partheniades, E., 1975. "An Investigation of the Depositional Properties of Flocculated Fine Sediments," Journal of Hydraulic Research, 13, No. 4, pp. 361-381.
- Orlanski, I., 1976. A Simple Boundary Condition for Unbounded Hyperbolic Flows, J. Computational Physics, 21:251-269.
- Parker, D.S., Kaufman, W.J. and Jenkins, D., 1972. "Floc Breakup in Turbulent Flocculation Processes," Journal of the Sanitary Engineering Division, Vol. 98, pp. 79-99.

- Partheniades, E., 1965. "Erosion and Deposition of Cohesive Soils," *Journal of the Hydraulics Division, Proceedings of the American Society of Civil Engineers*, Vol. 91, No. HY1, pp. 105-139.
- Partheniades, E., 1980. "Cohesive Sediment Transport Mechanics and Estuarine Sedimentation," lecture note from A Short Course on Engineering and Environmental Applications of Cohesive Sediment Studies, Coastal Engineering Archives, University of Florida, Gainesville.
- Pearson, R.A., 1974. Consistent Boundary Conditions for Numerical Models that Admit Dispersive Waves, *J. Atmospheric Sciences*, 31:1481-1489.
- Rayleigh, Lord, 1917. "On the Dynamics of Revolving Fluids." *Proceedings Royal Society, Series A*, Vol. 93, pp. 148-154.
- Saffman, P.G., and Turner, J.T., 1956. "On the Collision of Drops in Turbulent Clouds," *Journal of Fluid Mechanics*, Vol. 1, pp. 16-30.
- Sheng, Y.P. and Lick, W., 1979. "The Transport and Resuspension of Sediments in Shallow Lakes," *Journal of Geophysical Research*, Vol. 84, No. C4, pp. 1809-1826.
- Smolucowski, M., 1917. "Versuch einer Mathematischen Theorie der Koagulations-Kinetik Kolloid-Lösungen," *Zeitschrift für Physikalische Chemie*, Vol. 92, pp. 129-168.
- Tambo, N. and Watarabe, Y., 1979. "Physical Characteristics of Floccs-I. The Flocc Density Function and Aluminum Flocc," *Water Research*, Vol. 13, pp. 409-419.
- Tambo, N. and Hozumi, H., 1979. "Physical Characteristics of Floccs--II. Strength of Floccs," *Water Research*, Vol. 13, pp. 421-427.
- Taylor, G.I., 1923. "Stability of a Viscous Liquid Contained Between Two Rotating Cylinders," *Philosophical Transactions, Royal Society, Series A*, Vol. 223, pp. 289-345.
- Taylor, G.I., 1936. "Fluid Friction Between Rotating Cylinders," *Proceedings Royal Society, Series A*, Vol. 157, pp. 546-578.
- Tsai, C.H. and Lick, W., 1987. "Resuspension of Long Island Sound Sediments," *Conference on Coastal and Estuarine Pollution, Fukuoka, Japan*.
- Tsai, C.H. and Lick, W., 1986. "A Portable Device for Measuring Sediment Resuspension," *Journal of Great Lakes Research*, 12, No. 4, pp. 314-321.
- Tsai, C.H., S. Iacobellis and W. Lick, 1987. "The Flocculation of Fine-Grained Lake Sediments Due to a Uniform Shear Stress," *J. Great Lakes Research*, 13, No. 2, pp. 135-146.
- van Duuren, F.A., 1968. "Defined Velocity Gradient Model Flocculator," *Journal of the Sanitary Engineering Division, Proceedings of the American Society of Civil Engineers*, Vol. 94, No. SA4, pp. 671-682.

- Weber, W.J., Jr., 1972. "Physicochemical Processes for Water Quality Control," Wiley-Interscience, p. 68.
- Weiner, B.B., 1984. "Particle and Droplet Sizing Using Fraunhofer Diffraction," in Modern Methods of Particle Size Analysis, ed. H.G. Barth, John Wiley & Sons, pp. 135-172.
- Ziegler, C.K. and Lick, W., 1986. "A Numerical Model of the Resuspension, Deposition and Transport of Fine-Grained Sediments in Shallow Water," UCSR Report.
- Ziegler, C.K. and W. Lick, 1987. "Resuspension, Deposition, and Transport of Fine-Grained Sediments," Proceedings of the International Conference on Fluid Mechanics, Beijing, China.
- Ziegler, C.K. and W. Lick, 1988. "The Transport of Fine-Grained Sediments in Shallow Waters," Journal of Environmental Geology.